JPET Fast Forward. Published on July 30, 2013 as DOI: 10.1124/jpet.113.204735

JPET #204735

POSITIVE ALLOSTERIC MODULATION OF AMPA RECEPTORS FROM EFFICACY TO TOXICITY: THE INTERSPECIES EXPOSURE-RESPONSE CONTINUUM OF THE NOVEL POTENTIATOR PF-4778574

Christopher L. Shaffer, Raymond S. Hurst[1], Renato J. Scialis, Sarah M. Osgood, Dianne K. Bryce[2], William E. Hoffmann, John T. Lazzaro, Ashley N. Hanks, Susan Lotarski, Mark L. Weber, JianHua Liu, Frank S. Menniti[3], Christopher J. Schmidt and Mihály Hajós[4]

Department of Pharmacokinetics, Pharmacodynamics and Metabolism (C.L.S., R.J.S., S.M.O., J.L.) and the Neuroscience Research Unit (R.S.H., D.K.B., W.E.H., J.T.L., A.N.H., S.L., M.L.W., F.S.M., C.J.S., M.H.), Worldwide Research and Development, Groton Laboratories, Pfizer Inc., Groton, CT 06340

JPET Fast Forward. Published on July 30, 2013 as DOI: 10.1124/jpet.113.204735
This article has not been copyedited and formatted. The final version may differ from this version.

Running Title: The Exposure-Response Continuum of an AMPAR Potentiator

Address correspondence to:

Dr. Christopher L. Shaffer
Neuroscience Research Unit
Pharmacokinetics, Dynamics and Metabolism
Worldwide Research and Development
Pfizer Inc.
700 Main Street
Cambridge, MA 02139
Tel. 617.395.0769
Fax 860.686.6532
Email: Christopher.L.Shaffer@pfizer.com

Text pages: 36
Tables: 3
Figures: 6
References: 50
Words in Abstract: 244
Words in Introduction: 746
Words in Discussion: 1,490

Abbreviations: AMPA, α-amino-3-hydroxy-5-methyl-4-isoxazolepropionic acid; AUC, area under the plasma compound concentration-time curve; $C_{b,u}$, unbound brain compound concentration; $C_{b,u}$:$C_{p,u}$, unbound brain compound concentration-to-unbound plasma compound concentration ratio; ES, embryonic stem; HEK, human embryonic kidney; NMDA, *N*-methyl-D-aspartate; PF-4778574, *N*-{(3*R*,4*S*)-3-[4-(5-cyano-2-thienyl)phenyl]tetrahydro-2*H*-pyran-4-yl}propane-2-sulfonamide; PFC, prefrontal cortex; PPF, paired-pulse facilitation; SDR, spatial delayed response; TI, therapeutic index.

Recommended Section Assignment: Neuropharmacology

Abstract

α-Amino-3-hydroxy-5-methyl-4-isoxazolepropionic acid (AMPA) receptor (AMPAR) positive allosteric modulation (i.e. "potentiation") has been proposed to overcome cognitive impairments in schizophrenia, but AMPAR overstimulation can be excitotoxic. Thus, it is critical to define carefully a potentiator's mechanism-based therapeutic index (TI) and to determine confidently its translatability from rodents to higher-order species. Accordingly, the novel AMPAR potentiator *N*-{(3*R*,4*S*)-3-[4-(5-cyano-2-thienyl)phenyl]tetrahydro-2*H*-pyran-4-yl}propane-2-sulfonamide (PF-4778574) was characterized in a series of in vitro assays and single-dose animal studies evaluating AMPAR-mediated activities related to cognition and safety to afford an unbound brain compound concentration ($C_{b,u}$)-normalized interspecies exposure-response relationship. Since it is unknown which AMPAR subtype(s) may be selectively potentiated for an optimal TI, PF-4778574 binding affinity and functional potency were determined in rodent tissues expected to express a native mixture of AMPAR subunits and their associated proteins to afford composite pharmacologic values. Functional activity was also quantified in recombinant cell lines stably expressing human GluA2 flip or flop homotetramers. Pro-cognitive effects of PF-4778574 were evaluated in both rat electrophysiological and nonhuman primate (nhp) behavioral models of pharmacologically induced *N*-methyl-D-aspartate receptor hypofunction. Acute safety studies assessed cerebellum-based AMPAR activation (mouse) and motor coordination disruptions (mouse, dog and nhp), as well as convulsion (mouse, rat and dog). The resulting empirically derived exposure-response continuum for PF-4778574 defines a single-dose-based TI of 8-to-16-fold for self-limiting tremor, a readily monitorable

JPET Fast Forward. Published on July 30, 2013 as DOI: 10.1124/jpet.113.204735
This article has not been copyedited and formatted. The final version may differ from this version.

clinical adverse event. Importantly, the $C_{b,u}$ mediating each physiological effect were highly consistent across species with efficacy and convulsion occurring at just fractions of the in vitro-derived pharmacologic values.

Introduction

α-Amino-3-hydroxy-5-methyl-4-isoxazolepropionic acid (AMPA) receptors (AMPARs) mediate fast glutamatergic excitatory neurotransmission throughout the central nervous system. Changes in AMPAR density and subunit composition are principal mechanisms for the dynamic regulation of synaptic efficacy underlying adaptive brain functions (Malinow and Malenka, 2002). Consequently, AMPAR modulation has been targeted to treat numerous psychiatric and neurological diseases (O'Neill et al., 2004; Zarate Jr. and Manji, 2008). AMPAR-centric drug discovery (Black, 2005; Grove et al., 2010) has primarily focused on receptor activation via positive allosteric modulators (i.e. "potentiators") that tend to better match the degree and/or duration of AMPAR opening to synaptic activity than orthosteric agonists. Nonetheless, excessive AMPAR stimulation can cause degeneration of Purkinje cells and hippocampal neurons (Garthwaite and Garthwaite, 1991) and/or convulsion (Yamada, 1998). Therefore, it is imperative to understand the AMPAR potentiator exposures eliciting desired versus deleterious effects to identify a safe and well-tolerated molecule for high-confidence clinical evaluation. Because the effect of variations in AMPAR subtypes, splice variants and binding partners on a potentiator's therapeutic index (TI) is unknown, as is how the TI may vary across the mammalian hierarchy, a meticulous interspecies exposure-response relationship was developed for the novel AMPAR potentiator *N*-{(3*R*,4*S*)-3-[4-(5-cyano-2-thienyl)phenyl]tetrahydro-2*H*-pyran-4-yl}propane-2-sulfonamide (PF-4778574, Figure 1) (Estep et al., 2008). This exposure-response approach is grounded in both the "free drug" hypothesis (Tillement et al., 1988), which stipulates that interstitial fluid potentiator concentrations (C_{ISF}) dictate its interaction with the extracellular ligand

binding domains of AMPARs (Shaffer, 2010), and unbound brain compound concentration ($C_{b,u}$) being a valid C_{ISF} surrogate (Liu et al., 2009; Doran et al., 2012).

For this work, PF-4778574 efficacy was conceptually rooted in AMPAR potentiation overcoming certain cognitive impairments in schizophrenia (Millan et al., 2012; Moghaddam and Javitt, 2012; Collingridge et al., 2013). This rationale stems from the hypothesis that schizophrenia fundamentally results from dysfunction in *N*-methyl-D-aspartate receptor (NMDAR) glutamatergic neurotransmission (Olney and Farber, 1995; Goff and Coyle, 2001; Javitt, 2007). Clinical studies (Krystal et al., 1994; Javitt, 2007) in which healthy volunteers receiving acute subanesthetic doses of non-selective NMDAR antagonists (e.g. ketamine) presented with schizophrenia-like symptoms, including working memory deficits, support this proposition. Activated AMPARs depolarize neuronal membranes to relieve the Mg^{2+}-block of co-localized NMDARs, which increases NMDAR-mediated Ca^{2+}-gating (Lynch, 2002) to ultimately produce changes in the synaptic morphology and function (Malinow and Malenka, 2002; Lynch and Gall, 2006) believed to underlie learning and memory (Morris, 2003). Moreover, one chief mechanism of NMDAR-dependent increases in synaptic activity is AMPAR insertion into the synapse (Sun et al., 2005). Thus, potentiating AMPARs enhances NMDAR-induced synaptic potentiation. These facts, coupled with decreased AMPAR density in the schizophrenic hippocampus (Meador-Woodruff and Healy, 2000), suggest augmenting AMPAR activity may assuage cognitive disruptions in schizophrenia. Indeed, AMPAR potentiators have shown pro-cognitive properties in multiple preclinical models of hippocampal/cortical function and working memory (Black, 2005) and small clinical trials (Marenco and Weinberger, 2006).

Appreciating these collective concepts, PF-4778574 was characterized in a series of in vitro and single-dose in vivo assays assessing AMPAR-contingent activities related to nootropism and safety. Native AMPARs are tetrameric complexes comprised of multiple combinations of four monomeric subunits (GluA1–4), each having flip (i) and flop (o) isoforms, that are influenced by transmembrane proteins; this complexity is hypothesized to affect the functional heterogeneity of AMPAR-mediated synaptic transmission (Parsons et al., 2005; Arai and Kessler, 2007). Since it is unknown which AMPAR subtype(s) should (and/or can) be selectively potentiated for an optimal TI, PF-4778574 binding affinity was determined in primary rat cortical tissue while functional potency was assessed in both mouse embryonic stem (ES) cell-derived neurons (McNeish et al., 2010) and primary cultures of rat cortical neurons as these matrices are expected to express a native mixture of AMPAR subunits and their associated proteins to afford composite pharmacologic values. Functional activity was also quantified in recombinant cell lines stably expressing human GluA2i and GluA2o since other AMPAR potentiators interact with residues within these flip/flop domains (Fleming and England, 2010; Harms et al., 2013). For efficacy, PF-4778574 was evaluated in two contemporary animal models of pharmacologically induced NMDAR hypofunction (Olney et al., 1999): MK-801-induced subiculum-medial prefrontal cortex (PFC) dysfunction in rats (Kiss et al., 2011b) and ketamine-mediated spatial working memory impairment in nonhuman primates (nhp) (Roberts et al., 2010). Acute safety studies with PF-4778574 looked for cerebellum-based AMPAR activation (mouse) and motor coordination disruptions (mouse, dog and nhp), as well as convulsion (mouse, rat and dog). The resulting empirically derived $C_{b,u}$-normalized exposure-response continuum for PF-4778574

defines acceptable separation between drug concentrations associated with efficacy, motor coordination disruptions and convulsion.

JPET Fast Forward. Published on July 30, 2013 as DOI: 10.1124/jpet.113.204735
This article has not been copyedited and formatted. The final version may differ from this version.

Materials and Methods

Chemicals, Reagents and Animals. PF-4778574 (>99% chemical purity, 100% ee; Supplemental Data) (Estep et al., 2008) and *N*-((*S*)-1-(3,5-[^{3}H]-2-fluoro-4-((*S*)-5-((1-methylethylsulfonamido)methyl)-4,5-dihydroisoxazol-3-yl)phenyl)pyrrolidin-3-yl)acetamide ([^{3}H]PF-04725379, 98.5% radiochemical purity, 100% ee, 49 Ci/mmol) (Patel et al., submitted for publication) were synthesized and fully characterized by Neuroscience Chemistry at Pfizer Worldwide Research and Development (WRD, Groton, CT). PF-4778574 (Product No. PZ0214) is commercially available from Sigma-Aldrich Corporation (St. Louis, MO). Chemicals and solvents of reagent or HPLC grade were supplied by Sigma-Aldrich Corporation, Thermo Fisher Scientific (Waltham, MA) and Mallinckrodt Baker, Inc. (Phillipsburg, NJ). For control matrices, species-specific plasma was obtained from Bioreclamation, Inc. (Hicksville, NY) and rat brain tissue was obtained at WRD. Male CD-1 mice and Sprague-Dawley rats were bought from Harlan Laboratories (Indianapolis, IN) or Charles River Laboratories, Inc. (Wilmington, MA), male C57BL/6J mice were procured from The Jackson Laboratory (Bar Harbor, ME) and beagle dogs were sourced from Marshall BioResources (North Rose, New York). Non-naïve cynomolgus monkeys (*Macaca fascicularis*) resided within the WRD nhp colony (Groton, CT). All animal studies were performed in accordance with the *Guide for the Care and Use of Laboratory Animals* (Institute of Laboratory Animal Resources, 1996) using protocols reviewed and approved by the WRD Institutional Animal Care and Use Committee. All blood samples were collected into EDTA-containing tubes and processed immediately to obtain plasma, and the collection of neuromatrices from

JPET Fast Forward. Published on July 30, 2013 as DOI: 10.1124/jpet.113.204735
This article has not been copyedited and formatted. The final version may differ from this version.

rodents followed published techniques (Doran et al., 2012). All biomatrices collected for PF-4778574 quantification were stored at -70 °C until processing for bioanalysis.

In Vitro Pharmacology. ***Binding Affinity.*** *Rat Brain Homogenate Radioligand Binding Assay*. Rat brains were purchased from Pel-Freez® Biologicals (Rogers, AR). Cortex was dissected, homogenized using a polytron in 50 mM Tris 7.4 and centrifuged (40,000*g* for 20 min). The resulting pellet was resuspended in 50 mM Tris 7.4 and centrifuged (40,000*g* for 20 min); this was repeated three times, after which the pellet was resuspended in 30 mM Tris 7.4 (100 mg/mL) and stored at -80 °C. From a DMSO stock solution (10 or 30 mM), PF-4778574 was titrated then added (25 µL/well) at 10-fold its final concentration to a 96-well polypropylene plate containing assay buffer (30 mM Tris HCl, pH 7.4) supplemented with L-glutamic acid (25 µL, 5 mM). The AMPAR potentiator *N*-((3*R*,4*S*)-3-(2'-cyanobiphenyl-4-yl)tetrahydro-2*H*-pyran-4-yl)propane-2-sulfonamide (PF-4697190; 100 µM in assay buffer) (Estep et al., 2008; Shaffer et al., 2012) was added to positive control wells for a final concentration of 10 µM. To each well was added an aliquot (175 µL) of a 1 nM stock solution of [^{3}H]PF-04725379; for each experiment the precise stock solution concentration was determined by liquid scintillation counting. Previously prepared rat cortical tissue was thawed and homogenized (100 mg/mL) before its addition (25 µL, 2.5 mg tissue) to each sample well. Plates were incubated for 2 h at 37 °C and then harvested onto uncoated Filtermat B filters (PerkinElmer Inc., Waltham, MA) using a Skatron filter harvester (Skatron Instruments Ltd, Newmarket, UK) and Tris wash buffer (50 mM, pH 7.4, 4 °C). Filters were dried overnight, placed in scintillant bags and read on a Betaplate filtermat reader (PerkinElmer Inc.). Concentration-response data were fitted with a logistic function

JPET Fast Forward. Published on July 30, 2013 as DOI: 10.1124/jpet.113.204735
This article has not been copyedited and formatted. The final version may differ from this version.

using a four parameter logistic model. The K_i was determined using the ligand concentration of each experiment using the Cheng-Prusoff equation. Geometric means, rounded to two significant figures, and standard errors of the K_i values were calculated from multiple experiments.

Functional Activity. *Fluorimetric Imaging Plate Reader (FLIPR) Functional Assays.* Two distinct cell-based FLIPR functional assays were used for compound assessment: mouse ES cell-derived neuronal precursors and recombinant human cell lines. The ES cell-based assay has been fully disclosed (McNeish et al., 2010), thus only the recombinant cell lines are described here. Final DMSO concentrations were <1% in all assays.

Recombinant Human Cell Lines. HEK293 cell lines stably expressing the human AMPAR subunits GluA2i or GluA2o, both expressed in the Ca^{2+}-permeable Q form, were used (Invitrogen, Grand Island, NY). Cells were maintained in growth media containing DMEM High Glucose (500 mL, Gibco #10569-010), 10% dialyzed FBS (Gibco #26400-044), HEPES (Gibco #15630, 25 mM), MEM NEAA (Gibco #11140), Pen Strep (Gibco #15140, 100 μg/mL) and blasticidin (Invitrogen #R210-01, 50 μg/mL). Cells were maintained at 37 °C and 5% CO_2. Two days prior to the assay, cells were lifted from flasks with 0.25% trypsin and plated at a density of 12,500 cells/well on poly-D-lysine-coated black/clear 384-well plates (BD Biosciences, San Jose, CA).

FLIPR Methods. Assay buffer, containing 145 mM NaCl, 5 mM KCl, 10 mM glucose, 10 mM HEPES, 1 mM $MgSO_4$ and 2 mM $CaCl_2$ and pH adjusted to 7.4 with 1 M NaOH, was freshly prepared for each experiment. A Fluo-4 AM (Invitrogen) stock solution (1 mM in DMSO with 10% pluronic acid) was added to DMEM for a 4 μM dye

JPET Fast Forward. Published on July 30, 2013 as DOI: 10.1124/jpet.113.204735
This article has not been copyedited and formatted. The final version may differ from this version.

incubation media, which was then supplemented with probenecid (2.5 mM, Sigma). Probenecid-containing (2.5 mM) assay buffer was also used for cell washing, but not compound preparation. Following growth media removal from cell plates, dye solution (50 μL) was added to each well. Plates were then incubated for 1 h at room temperature (rt) before the dye solution was removed and washed three times with assay buffer, leaving 30 μL assay buffer/well. Plates were left at rt for at least 10 min before adding compound. The FLIPR (Molecular Devices, LLC, Sunnyvale, CA) was used to perform simultaneous Ca^{2+} imaging and drug application. Compounds were initially dissolved in DMSO (10 or 30 mM). After initial compound titration, the compound drug plate was prepared in assay buffer at 4-fold the final concentration. PF-4778574 (15 μL/well) was transferred from the drug plate to the cell plate while imaging the entire 384-well plate at a rate of 1 sample/2 s. Five and 40 samples were recorded before and after compound addition, respectively, using excitation and emission wavelengths of 488 and 510 to 570 nm, respectively. After the first read, the plate was incubated at rt for 10 min, then placed in the FLIPR for a second addition, during which a 4-fold challenge concentration of *S*-AMPA (15 μL/well) was added to the cell plate while imaging. The compound addition and read protocol for the second addition was the same as the first. A final *S*-AMPA concentration of 32 μM was used for the assay. The peak fluorescence in each well was determined by subtracting the maximal fluorescence across the 40 samples after compound addition from the baseline fluorescence. Data analysis for the second addition was performed by determining the percent effect at each concentration using a reference AMPAR potentiator as the positive control and *S*-AMPA alone as the negative control. A maximal concentration of the potentiator cyclothiazide (10 or 32 μM; Tocris

JPET Fast Forward. Published on July 30, 2013 as DOI: 10.1124/jpet.113.204735
This article has not been copyedited and formatted. The final version may differ from this version.

Bioscience, Bristol, UK) was used as the positive control for the mouse ES cell-derived neurons. Maximal concentrations (32 μM) of the potentiators PF-4697190 (Estep et al., 2008; Shaffer et al., 2012) or 2-(2-(3-(trifluoromethyl)-4,5,6,7-tetrahydro-1*H*-indaol-1-yl)acetamido)-4,5,6,7-tetrahydrobenzo[b]thiophene-3-carboxamide (CE-382349) (McNeish et al., 2010) were used as positive controls for the human GluA2 cell lines. Concentration-response data were fit as described beforehand. Geometric means, rounded to two significant figures, and standard errors of the EC_{50} values were calculated from multiple experiments. The percent efficacy in each experiment was determined by dividing the maximum asymptote of the fitted PF-4778574 curve by the positive control in the assay. Average percent efficacy was calculated as an arithmetic mean ± standard error of the mean (SEM).

Rat Cortical Neurons Electrophysiological Studies. Rat fetal (E18) frontal cortex primary neurons were grown on 12 mm round poly-D-lysine-coated cover slips (ca. 1×10^5 cells/well plated two to three weeks prior to recording in 12-well tissue culture plates). Cover slips with primary neurons were placed in a recording chamber and superfused (ca. 1 to 2 mL/min) with external buffer containing (in mM) NaCl (130), KCl (2), $MgCl_2$ (1.5), $CaCl_2$ (2), HEPES (10) and glucose, pH 7.4 and ca. 305–310 mOsM at rt. One millimeter O.D. glass electrodes were filled with internal solution containing (in mM) $CsCH_3SO_3$ (126), CsCl (10), NaCl (4), $MgCl_2$ (1), EGTA (8), $CaCl_2$ (0.5), HEPES (10), Na_2ATP (3), NaGTP (0.3) and phosphocreatine (4), pH 7.2 and ca. 295 mOsM, and had a tip resistance of 3–4 MΩ. Patch clamp experiments were conducted at rt using an Axoclamp 200B amplifier (Molecular Devices, LLC) in the whole-cell configuration. Using a pCLAMP 10 software (Molecular Devices, LLC) protocol, cell membrane

potential was voltage-clamped at -60 mV. For *S*-AMPA (±300 nM PF-4778574) concentration-response studies, it was added in increasing concentration (0.1, 0.3, 1, 3, 10, 30 and 100 μM) to elicit a current. Four-second compound applications were made via gravity feed using a 3-barreled glass tube connected to a SF-77B fast step perfusion system (Warner Instruments LLC, Hamden, CT) with a 120 s washout period between applications. For PF-4778574 concentration-response experiments, *S*-AMPA (30 μM) with increasing PF-4778574 concentrations (3, 30, 300 and 3000 nM) were added using 20 s applications with a 120 s washout period between applications. Data were calculated as % maximum current (for *S*-AMPA concentration-response) or % *S*-AMPA control current (for PF-4778574 concentration-response), and EC_{50} were calculated using a logistic non-linear regression fit. Data were analyzed and visualized using Clampfit 10 software (Molecular Devices, LLC).

Pharmacokinetics Studies. ***Plasma and Brain Homogenate Nonspecific Binding.*** Using a reported (Doran et al., 2012) equilibrium dialysis procedure, the unbound fraction (f_u) of PF-4778574 (1 μM, N=3/species) was determined in CD-1 mouse, Sprague-Dawley rat, beagle dog and cynomolgus monkey plasma ($f_{u,p}$) and Sprague-Dawley rat brain homogenate ($f_{u,b}$). The stability of PF-4778574 in each matrix and the optimal dialysis time were determined separately prior to actual studies.

In Vivo Pharmacokinetics. Before in vivo pharmacology experiments, studies with PF-4778574 characterizing its pharmacokinetics (peripheral and/or central) were conducted in the relevant preclinical species. These studies determined: plasma (C_p) and/or brain (C_b) compound concentrations at select times after a specific dose; pharmacokinetic parameters (particularly maximal matrix PF-4778574 concentration

(C_{max}) and AUC) and their linearity at doses of pharmacological interest, which allowed the correlation of pharmacodynamics to C_p and/or C_b; the first time of C_{max} (T_{max}), which determined PF-4778574 pretreatment time in certain assays; and, PF-4778574 plasma half-life ($t_{1/2}$) that dictated wash-out periods between doses in the nhp spatial delayed response (SDR) task. Individual animal doses were calculated based on respective dose solution concentrations (mg/mL), pretreatment body weights (kg) and dose volume (mL/kg). The actual amount of dose solution administered to each animal was determined by weighing the loaded syringe before and after it was dispensed. All study animals were fasted overnight and for ca. 4 h post-dose. For each species, the specific vehicle and dosing route used in its pharmacokinetics study were also utilized in its pharmacodynamics experiment.

Mouse. A single dose (0.178 mg/kg) of PF-4778574 in 5:5:90 (v/v/v) DMSO:cremophor EL:deionized H_2O (0.0178 mg/mL) was administered (10 mL/kg) subcutaneously (SC) to CD-1 (N=2) or C57BL/6J (N=3) mice. At 0.5 h post-dose, animals were placed under isoflurane anesthesia for the collection of blood and brain samples.

Rat. Intravenous Dose. From jugular vein-cannulated Sprague-Dawley rats (N=3) receiving a single bolus (1 mL/kg) intravenously (IV) of PF-4778574 (0.2 mg/kg) in 2:98 (v/v) DMSO:20% hydroxypropyl-β-cyclodextrin (0.2 mg/mL), blood samples (0.5 mL) were serially collected just before dosing and at 0.083, 0.167, 0.25, 0.5, 1, 2, 4, 6, 8 and 12 h post-dose. *Neuropharmacokinetics.* As described (Doran et al., 2012), a single dose (1 mg/kg, SC) of PF-4778574 in 2:98 (v/v) DMSO:20% hydroxypropyl-β-cyclodextrin (1 mg/mL) was injected (1 mL/kg) into each male Sprague-Dawley rat. Blood,

JPET Fast Forward. Published on July 30, 2013 as DOI: 10.1124/jpet.113.204735
This article has not been copyedited and formatted. The final version may differ from this version.

cerebrospinal fluid (CSF) and brain samples were collected from each animal after euthanasia by CO_2 asphyxiation at 0.25, 0.5, 1, 2, 4 and 8 h post-dose (N=2/time point).

Dog. A single dose (0.1 mg/kg) of PF-4778574 in 0.5% methylcellulose (0.1 mg/mL) was given (1 mL/kg) orally (PO) to each dog (N=1/gender). Blood samples (2 mL) were obtained via the jugular vein just before dosing and at 0.25, 0.5, 1, 2 and 4 h post-dose. During this time period, dogs were continuously monitored by trained lab staff for any readily apparent adverse events.

Nonhuman primate (nhp). A single dose (0.1 or 0.32 mg/kg, SC) of PF-4778574 in 1:9 (v/v) cremophor EL:deionized H_2O (0.3 or 1 mg/mL) was administered (0.33 mL/kg delivered to the dorsal thoracolumbar area) to each nhp (N=2/dose). Blood samples (3 mL) were obtained via a vascular access port just before dosing and at 0.25, 0.5, 1, 2, 4, 6 and 24 h post-dose. After remaining chaired for 2 h post-dose, animals were returned to their home cage. They were again chaired just prior to blood collection at 4, 6 and 24 h post-dose, and released back to their home cage after each blood sampling. Trained lab staff constantly observed each nhp for any readily apparent adverse events for 6 h post-dose.

Quantitative Analysis of PF-4778574 in Biological Matrices. The quantification of PF-4778574 in plasma, CSF or brain tissue samples from rodents, dogs or nhp was achieved using published LC-MS/MS methodologies (Doran et al., 2012). The dynamic ranges were 0.488 to 500 ng/mL for plasma samples and 0.488 to 1000 ng/mL for CSF and brain tissue samples.

Pharmacokinetic Calculations. Pharmacokinetic parameters were calculated by non-compartmental analyses using WinNonlin version 5.2 (Pharsight Corp., Mountain View,

JPET Fast Forward. Published on July 30, 2013 as DOI: 10.1124/jpet.113.204735
This article has not been copyedited and formatted. The final version may differ from this version.

CA). The area under the plasma compound concentration-time curve ($AUC_{0–Tlast}$) was calculated using the linear trapezoidal method, the elimination rate constant (k_{el}) was determined by linear regression of the log concentration versus time data during the last observable elimination phase, half-life ($t_{1/2}$) was calculated as $0.693/k_{el}$, and $AUC_{0–\infty}$ was calculated as the sum of $AUC_{0–Tlast}$ and $AUC_{Tlast–\infty}$, which was determined by dividing the C_p at T_{last} by k_{el}. Both C_{max} and T_{max} were taken directly from the matrix compound concentration versus time data. Means and standard deviations (SD) were computed when half or greater of the values exceeded 0.488 ng/mL. A value of 0 was used if a measured value was <0.488 ng/mL. Volume of distribution (V) was calculated by the equation $V = CL \bullet (AUMC/AUC)$, where AUMC is the total area under the first moment-time curve and systemic clearance (CL) was determined by dividing the measured dose by plasma $AUC_{0–\infty}$. All AUC values were subject weight-normalized.

In Vivo Pharmacology. PF-4778574 was studied in select in vivo pharmacology models to understand the relationship between its $C_{b,u}$ and a particular AMPAR-mediated effect, which together allowed comparison to its in vitro pharmacology values. Collectively, this strategy provided dose-dependent, temporally normalized and assay-dependent $C_{b,u}$ that could be directly compared across all in vivo models. For each species, its pharmacodynamics evaluation used the same dosing vehicle, volume and route as its pharmacokinetics studies. For terminal assays in which brain tissue was collected from an animal undergoing the assessment, $C_{b,u}$ (nM units) was determined by measured C_b, PF-4778574 molecular weight (MW, 390.5 g/mol), rat $f_{u,b}$, an assumed brain tissue density of 1 g/mL and Eq. 1:

JPET Fast Forward. Published on July 30, 2013 as DOI: 10.1124/jpet.113.204735
This article has not been copyedited and formatted. The final version may differ from this version.

$$(C_b / \mathrm{MW}) \bullet 1000 \bullet f_{u,b} = C_{b,u} \qquad (1)$$

The experimentally determined rat $f_{u,b}$ was used for mouse $C_{b,u}$ calculations since interspecies $f_{u,b}$ are highly consistent (Di et al., 2011).

For non-terminal assays, if plasma samples were collected for PF-4778574 quantification during the evaluation (e.g. low dose dog studies) then $C_{b,u}$ was projected from each C_p using compound MW, species-specific $f_{u,p}$, species-specific unbound brain compound concentration-to-unbound plasma compound concentration ratio ($C_{b,u}$:$C_{p,u}$) (Doran et al., 2012) and Eq. 2:

$$(C_p / \mathrm{MW}) \bullet 1000 \bullet f_{u,p} \bullet (C_{b,u}:C_{p,u}) = C_{b,u} \qquad (2)$$

If plasma samples were not collected for PF-4778574 quantification in the pharmacodynamic test (e.g. nhp SDR task) then C_p at any time point for a specific dose within that species' satellite pharmacokinetics study was converted to $C_{b,u}$ using Eq. 2. The resulting $C_{b,u}$ versus time data were then used to extrapolate linearly $C_{b,u}$ at a specific time point for each dose tested in the in vivo pharmacology model.

Mechanism. *Mouse Cerebellum Cyclic Guanosine Monophosphate (cGMP) Assay*. Paralleling the procedure of Ryder *et al.* (2006), adult male CD-1 mice (25–30 g, acclimated to the vivarium 7 d before use, N=5–6/dose) receiving vehicle or PF-4778574 (0.1, 0.32 or 1.0 mg/kg, SC) were placed in an open shoebox with sawdust bedding and observed for 0.5 h. Mice were then individually placed head first in a Plexiglas restraining device and euthanized using a beam of microwave radiation focused on the

skull for 0.88 s at 100% power in a Cober Electronics microwave (Cober Electronics, Inc., Norwalk, CT). After cooling for 1 min, the cerebellum was dissected, weighed and frozen on dry ice. Tissue cGMP levels were determined using a competitive enzyme immunoassay (EIA) using a commercially available Cyclic GMP EIA kit (Cayman Chemical Company, Ann Arbor, MI). All buffers and cGMP standards were prepared exactly as described in the package insert. Each cerebellum sample was homogenized (10 μL buffer/mg tissue) in lysis buffer (10 mM Tris HCl, 100 mM NaCl, 1 mM EDTA and 0.3% NP-40, pH 7.4) using a tip sonicator. Homogenate was added to a 1.5 mL Eppendorf tube and centrifuged (18,000*g* for 20 min at 4 °C), and the supernatant was diluted 1:25 with EIA buffer and added in triplicate to a 96-well plate. Samples were processed according to kit directions for 12 h at 4 °C. A cGMP standard curve (0.023 to 3.0 pmol/mL) was included on each assay plate. Following incubation, plates were washed, developed using Ellman's reagent for 2 h at rt, and then read at 420 nm on a SpectraMax Microplate Reader (Molecular Devices, LLC). Data were compiled and reduced using the SpectraMax data reduction software, which calculates sample cGMP levels via standard curve extrapolation. For each dose group, data were reported as group means ± SEM using X-fold changes in tissue cGMP levels relative to the vehicle-treated group. PF-4778574 doses were compared to the concurrent vehicle control group using One-way Analysis of Variance (ANOVA) followed by Dunnett's t-test (SigmaStat Version 3.5; Systat Software, Inc., Chicago, IL). A value of $P<0.05$ indicated a statistically significant effect.

Safety. *Mouse Rotarod Assay.* For two weeks prior to testing, C57BL/6J male mice (7 to 8 weeks old) were group-housed (N=4/isolator) with free access to food and water

in a temperature- and humidity-controlled environment on a 6 am/6 pm light/dark schedule. On Test Day 1, mice were acclimated to the test room 1 h prior to the training session. Four programmable SmartRod® chambers with SmartRod® software version 1.70 (AccuScan Instruments, Columbus, OH) were used for testing. Each chamber was equipped with a rotating rod (3 cm in diameter, spanned the 11 cm width of the chamber) horizontally affixed 32.5 cm on-center above the grid floor. Two infrared (IR) beams, located 2 cm above the floor, detected the animal when it fell from the rods and deactivated the timer to record automatically fall latency. Rods were programmed to accelerate at a rate of 0.25 rev/s to a maximum speed of 20 rpm over 62 s, after which the rod decelerated over an additional 5 s to the stop position. The maximum cycle time for one trial was 67 s. The training session consisted of six consecutive trials on the rod with a 10 s inter-trial interval (ITI) for each mouse. Mice had to complete two of the six training trials with a fall latency >10 s to be accepted for testing the following day. Mice that did not meet the criteria were eliminated from the study, and mice that met the criteria were returned to their home cage and remained in the test room under conditions consistent with the housing room environment. On Test Day 2, mice were randomly assigned to groups of 12 and dosed with vehicle or PF-4778574 (0.178, 0.032 or 0.56 mg/kg, SC). For testing, each mouse was subjected to three consecutive trials on the rods with a 10 s ITI. The mean fall latency for three trials was calculated and data were reported as group means ± SEM. PF-4778574 doses were compared to the concurrent vehicle control group using One-way ANOVA followed by Dunnett's t-test (SigmaStat Version 3.5; Systat Software, Inc.). A value of $P<0.05$ indicated a statistically significant effect.

Convulsion Dose-Response Studies. Rodents. PF-4778574 was administered (N=6/dose) to adult male CD-1 mice (1, 1.78 or 3.2 mg/kg, SC) or Sprague-Dawley rats (1.78, 3.2 or 5.6 mg/kg, SC), which were observed for up to 2 h post-dose. Individual animals were euthanized by CO_2 asphyxiation at the time of convulsion (if any), and blood and brain were collected for PF-4778574 quantification. *Dogs.* These studies were conducted in the department of Drug Safety and Research at WRD (Groton, CT) by scientists highly skilled in monitoring and treating serious adverse events in research animals. Adult beagle dogs were administered PF-4778574 (0.2 (N=1 female), 0.25 (N=1 male) or 0.5 (N=1/gender) mg/kg, PO) and observed from 0 to 4 h post-dose. Blood samples (2 mL) were scheduled for collection at 0.25, 0.5, 1, 2 and 4 h post-dose. In the event of a convulsion, a blood sample was taken at the time of its first observation.

Efficacy. *Rat MK-801-Disrupted Cortical Oscillation and Paired-Pulse Facilitation (PPF) Assay.* The objective of this study was to quantify the effects of systemically administered PF-4778574 on the cortical disruption of electroencephalogram (EEG) and paired-pulse facilitation (PPF) by the non-competitive NMDAR antagonist MK-801 in urethane-anesthetized Sprague-Dawley rats (Kiss et al., 2011). This is a preclinical model, which evaluates the subiculum-medial prefrontal cortex pathway, proposed for studying NMDAR hypofunction of schizophrenia. Experimental procedures were those published by Kiss *et al.* (2011) using male Sprague-Dawley rats (250 to 320 g, N=5) under urethane anesthesia (1.5 mg/kg, intraparotenial). For the IV dose-response effects of PF-4778574, control waveform averages were first computed using 60 consecutive paired-stimuli over a 10 min period. MK-801 (0.05 mg/kg, IV; Tocris Bioscience, Bristol, UK) was then administered, and, after a 5-min waiting period, paired-pulse

averaging was again conducted over the next two consecutive 5-min time bins. The total MK-801 response was then computed by combining these two averages. At the end of the second 5-min data collection time bin (i.e. 15 min after MK-801 injection), cumulative IV administration of PF-4778574 (0.03 and 0.1 mg/kg) was initiated. Similar to how the data were handled following MK-801 dosing, 5 min were allowed between each successive PF-4778574 injection and the start of the subsequent averaging. If no effect was observed before the end of the second 5-min averaging period then the two 5-min averages were combined as a single value for that dose and the next IV dose was given. If an effect was observed at any point during the first two averages following a given dose, then two additional 5-min averages were combined as the data point for that dose. The reversal of the MK-801 effects by PF-4778574 did not occur in a typical cumulative dose-response manner, but rather as an all-or-none effect with variable threshold doses between animals. Since reversal was an all-or-none effect once the threshold dose in a particular animal was reached, no additional cumulative doses of PF-4778574 were given. Instead, responses to the paired-pulse stimulations were recorded continuously and averaged over each consecutive 10-min time-bin for 60 min to obtain the overall time course of PF-4778574 activity. Mean effects in the PF-4778574 doses were compared to both the control and MK-801 doses using a two-tailed Student's *t* test (Microsoft Excel®, Microsoft Corporation, Redmond, WA). A value of $p<0.05$ indicated a statistically significant effect.

Nonhuman Primate Ketamine-disrupted Spatial Delayed Response (SDR) Task. The objective of this study was to quantify the effects of PF-4778574 on ketamine-induced spatial working memory impairments in nhp, a proposed model of cognitive impairment

associated with schizophrenia. PF-4778574 (0.001, 0.01 and 0.1 mg/kg, SC) was evaluated as already described (Roberts et al., 2010).

Results

In Vitro Pharmacology. Displacement studies using [^{3}H]PF-04725379 in rat cortical tissue determined a K_i of 85 nM for PF-4778574. Functional potency was assessed by measuring effects induced by *S*-AMPA alone and following PF-4778574 pretreatment using either changes in intracellular Ca^{2+} concentration (HEK293 cells and mouse ES cell-derived neuronal precursors) or whole-cell current (rat primary cortical neurons) to measure the *S*-AMPA-dependent responses. When added alone (up to 32 and 3 μM in the FLIPR-based assays and rat cortical neuron electrophysiological assay, respectively), PF-4778574 produced no detectable response in any of the tested cell types expressing functional AMPARs. However, PF-4778574 concentration-dependently increased *S*-AMPA-evoked responses in HEK293 cells expressing human GluA2i or GluA2o, mouse neuronal precursors and rat primary neurons. Depending on the cell type, PF-4778574 EC_{50} ranged from 45 to 919 nM. Table 1 summarizes the geometric means for pK_i, K_i, pEC_{50}, EC_{50}, the arithmetic means for percent efficacy and the number of assay replicates (*N*). Intrinsic efficacy was evaluated in primary cultures of rat cortical neurons using whole-cell patch clamp electrophysiology. When pre-applied to neurons, PF-4778574 increased the maximal *S*-AMPA-evoked current by ca. 9-fold at a maximally effective concentration (Figures 2A and 2C). PF-4778574 also increased the potency of *S*-AMPA for activating AMPARs; for example (Figure 2B), the EC_{50} of *S*-AMPA was shifted from 4.38 μM in the absence of PF-4778574 to 0.67 μM in the presence of 300 nM PF-4778574 (near its EC_{50} of 282 nM).

Pharmacokinetics Studies. Species-dependent single or multiple time point neuropharmacokinetics and/or pharmacokinetics studies were conducted prior to in vivo

JPET Fast Forward. Published on July 30, 2013 as DOI: 10.1124/jpet.113.204735
This article has not been copyedited and formatted. The final version may differ from this version.

pharmacology tests to optimize PF-4778574 dose selection and pharmacodynamic time point(s), as well as to ensure accurate $C_{b,u}$ extrapolation at select time points for those doses. All pharmacokinetics data are within Supplemental Data.

Plasma and Brain Homogenate Nonspecific Binding. PF-4778574 had consistently low $f_{u,p}$ for CD-1 mouse (0.0570), Sprague-Dawley rat (0.0476), beagle dog (0.0685) and cynomolgus monkey (0.0876), and a lower rat $f_{u,b}$ (0.0195). Due to $f_{u,b}$ being species independent (Di et al., 2011), the rat $f_{u,b}$ was used to convert mouse C_b to $C_{b,u}$.

Neuropharmacokinetics. *Mouse.* Thirty minutes after a single dose (0.178 mg/kg, SC) of PF-4778574, CD-1 mice had a mean C_p of 15.7 ng/mL and C_b of 18.8 ng/g (equating to a $C_{b,u}$ of 0.94 nM) resulting in a total brain-to-total plasma ratio (C_b:C_p) of 1.20 and a $C_{b,u}$:$C_{p,u}$ of 0.41. For the same time point and dose, C57BL/6J mice had a mean (±SD) C_p of 26.1±6.5 ng/mL and C_b of 30.5±6.6 ng/g (equating to a $C_{b,u}$ of 1.52±0.33 nM), which afforded a C_b:C_p of 1.27±0.63. Based on these data and the pretreatment time of 0.5 h in both the mouse cGMP and rotarod assays, doses within each model were assumed to have the same dose-$C_{b,u}$ relationship as in this pharmacokinetics study and, thus, their $C_{b,u}$ were extrapolated linearly from these data. *Rat.* Following a single dose (1 mg/kg, SC), PF-4778574 demonstrated similar $t_{1/2}$ within plasma (0.680 h), CSF (1.29 h) and brain (0.804 h), and a mean T_{max} within each neuromatrix of ca. 0.25 h post-dose (Figure 3A). Consistent with it being a highly permeable non-P-glycoprotein and non-breast cancer resistance protein substrate (internal Pfizer unpublished data), PF-4778574 afforded $AUC_{0-Tlast}$-derived ratios suggesting it is readily and rapidly brain penetrant (C_b:C_p of 1.07) with interneurocompartmental equilibrium, and a $C_{b,u}$:$C_{p,u}$ of 0.44 (Doran et al., 2012). *Dog and nhp.* In independently conducted

JPET Fast Forward. Published on July 30, 2013 as DOI: 10.1124/jpet.113.204735
This article has not been copyedited and formatted. The final version may differ from this version.

neuropharmacokinetics studies (Doran et al., 2012) in dogs (0.5 mg/kg, PO) and nhp (0.1 mg/kg, SC), PF-4778574 had C_b:C_p of 1.35 and 2.82 and $C_{b,u}$:$C_{p,u}$ of 0.51 and 0.73, respectively. Rodent and large animal $C_{b,u}$:$C_{p,u}$ were ≤1.7-fold different (Table 2).

Pharmacokinetics. *Rat.* After an IV bolus (0.2 mg/kg), PF-4778574 demonstrated very high *CL* (250 mL/min/kg) and *V* (4.59 L/kg) with a very short $t_{1/2}$ (0.237 h). Generated C_p versus time data were converted to $C_{b,u}$ versus time (Figure 3B) using Eq. 2, and this dose-$C_{b,u}$-time relationship was used to extrapolate linearly $C_{b,u}$ versus time for each dose evaluated in the rat PPF assay. *Dog.* Following administration of the highest dose (0.1 mg/kg, PO) not associated with any readily apparent untoward effects, PF-4778574 revealed moderate apparent *CL* (8.01 mL/min/kg), high apparent *V* (2.1 L/kg) and moderate $t_{1/2}$ (3.1 h), with mean C_{max} (56.0 ng/mL) at 0.75 h post-dose and $AUC_{0-\infty}$ of 210 ng•h/mL. Via Eq. 2, C_p versus time data were transformed to $C_{b,u}$ versus time (Figure 3C). The highest individual projected $C_{b,u}$ were 4.1 and 5.9 nM. *Nonhuman primate.* As reported (Roberts et al., 2010) for acute doses (0.1 and 0.32 mg/kg, SC), PF-4778574 had a moderate mean $t_{1/2}$ (3.36 h) with mean T_{max} occurring ca. 2 h post-dose; mean C_{max} (25.5 and 102 ng/mL, respectively) and $AUC_{0-\infty}$ (85.0 and 340 ng•h/mL, respectively) were linear with dose, suggesting stationary pharmacokinetics across this 3.2-fold dose range. Using Eq. 2, C_p versus time data were translated to $C_{b,u}$ versus time (Figure 3D), and this dose-$C_{b,u}$-time relationship was used for the linear projection of $C_{b,u}$ versus time for the doses evaluated in the nhp SDR model. PF-4778574 was innocuous at 0.1 mg/kg, but at 0.32 mg/kg movement-related tremors, ataxia and decreased activity were observed from ca. 2 to 4 h post-dose, consistent with its T_{max} and exposure plateau over this time period. Based on individual animal pharmacokinetics and the side-effects

observed at 0.32 mg/kg, SC, movement-related tremors and ataxia occurred in nhp at projected $C_{b,u}$ of 8.0 to 24.1 nM (Figure 4A).

In Vivo Pharmacology. PF-4778574 was assessed in select in vivo pharmacology models to define the relationship between its $C_{b,u}$ and AMPAR-mediated effects, and the cross-species translatability of these correlations. Holistically, this afforded a $C_{b,u}$-normalized interspecies exposure-response continuum for PF-4778574 across multiple models of AMPAR-dependent mechanism, safety and pro-cognitive properties ("efficacy") to quantify its acute-dose TI.

Mechanism. *Mouse Cerebellum cGMP Assay.* PF-4778574 dose-dependently increased cGMP levels in CD-1 mouse cerebellum with statistically significant elevations (versus vehicle-treated animals) 0.5 h after receiving doses of 0.32 ($p<0.05$) and 1.0 ($p<0.01$) mg/kg, SC (Figure 5A). Based on the satellite CD-1 mouse neuropharmacokinetics study (0.178 mg/kg, SC) and assuming stationary pharmacokinetics at all tested doses, the projected mean PF-4778574 $C_{b,u}$ at the cGMP-raising doses were 1.7 and 5.3 nM, respectively.

Safety. *Mouse rotarod assay.* PF-4778574 induced statistically meaningful ($p<0.05$) motor deficits in C57BL/6J mice undergoing an accelerating rotarod test 0.5 h after 0.56 mg/kg, SC (Figure 5B). Assuming a linear dose-exposure relationship across the doses evaluated, the C57BL/6J mouse neuropharmacokinetics study (0.178 mg/kg, SC) projected a mean PF-4778574 $C_{b,u}$ of 4.8 nM to decrease animal fall latency.

Convulsion Dose-Response Studies. Due to the concern of convulsions resulting from AMPAR potentiation and the necessity to understand both the consistency (if any) of interspecies convulsion-eliciting $C_{b,u}$ and their separation from those inducing other

effects, PF-4778574 underwent convulsion dose-response studies in CD-1 mice, Sprague-Dawley rats and beagle dogs. *Rodents.* In CD-1 mice, general convulsions were observed at both 1.78 (N=5 of 6 animals) and 3.2 (N=6/6) mg/kg, SC; animals receiving 1 mg/kg, SC had no readily apparent adverse events. Following dosing, convulsions occurred later (23±11 min) in the 1.78 mg/kg dose group than in the 3.2 mg/kg dose group (7±2 min), which is consistent with their concentration "threshold" nature. Mean (±SD) convulsion-causing $C_{b,u}$ were 9.6±0.9 nM and 13.2±4.9 nM in the 1.78 and 3.2 mg/kg groups, respectively. Including all convulsing animals (N=11), a $C_{b,u}$ of 11.6±4.0 nM was deemed the convulsive exposure threshold in CD-1 mice (Figure 4B). In rats, convulsions were observed in both the 3.2 (N=6/6) and 5.6 (N=5/6) mg/kg, SC groups; although no convulsions were observed at 1.78 mg/kg, SC, these animals (N=5/6) became stationary ca. 20 min post-dose. As in mice, convulsions occurred later (54±27 min) in the 3.2 mg/kg dose group than in the 5.6 mg/kg dose group (27±17 min). Mean (±SD) convulsion-causing $C_{b,u}$ were 10.7±1.5 nM and 11.8±1.9 nM in the 3.2 and 5.6 mg/kg groups, respectively. Collectively (N=11), a $C_{b,u}$ of 11.2±1.6 nM defined the convulsive exposure threshold in Sprague-Dawley rats (Figure 4B). *Dogs.* Doses were selected based on the initial dog pharmacokinetics study (0.1 mg/kg, PO) and rodent dose-convulsion work. Following 0.5 mg/kg, PO (N=2), the first dose tested, each animal experienced repetitive generalized convulsions at 14 and 18 min post-dose that dictated their euthanasia; C_p at these time points were 182 and 207 ng/mL, respectively, which, via Eq. 2 and the dog $C_{b,u}$:$C_{p,u}$ of 0.51 (Table 2), afford respective projected $C_{b,u}$ of 16.3 and 18.5 nM (Figure 4B). In the next dose (0.25 mg/kg, PO, N=1), whole-body tremors onset ca. 15 min (projected $C_{b,u}$ of 8.8 nM) after dosing and resolved by 1 h post-

JPET Fast Forward. Published on July 30, 2013 as DOI: 10.1124/jpet.113.204735
This article has not been copyedited and formatted. The final version may differ from this version.

dose ($C_{b,u}$ of 13.8 nM); ataxia was observed from ca. 15 min to 2 h post-dose ($C_{b,u}$ of 12.1 nM). Although these adverse events were self-limiting and the animal survived the dose, the severity of signs was considered dose-limiting for subsequent studies. Lastly, following 0.2 mg/kg, PO (N=1), whole-body tremors and ataxia presented from 0.5 to 2 h post-dose (projected $C_{b,u}$ of 10.9 to 6.0 nM) with signs being less severe than those observed in the 0.25 mg/kg animal. Taken together, in dogs PF-4778574 induced generalized tremors and ataxia from $C_{b,u}$ of 6.0 to 15.6 nM (Figure 4A) and convulsions at a mean $C_{b,u}$ of 17.4 nM (Figure 4B).

Efficacy. *Rat MK-801-Disrupted Cortical Oscillation and PPF Assay.* This study quantified the effects of PF-4778574 on the disruption of cortical EEG and PPF by the NMDAR antagonist MK-801 in urethane-anesthetized Sprague-Dawley rats (Kiss et al., 2011b). Consistent with prior data (Kiss et al., 2011a; Kiss et al., 2011b), MK-801 significantly altered EEG delta activity (i.e. the regular 2 Hz delta oscillation was changed to an irregular 0.5 to 1.5 Hz delta rhythm) while simultaneously reducing PPF elicited by electrical stimulation of the subiculum; these MK-801-mediated effects were both sustained for 1 h post-dose and unaffected by an IV bolus of vehicle. Intravenous administration of PF-4778574 at 0.1 mg/kg, but not 0.03 mg/kg, significantly reversed the MK-801-induced increase in the low delta component of the local field potential and decrease in PPF (Figure 6). After the 0.1 mg/kg bolus, these significant effects of PF-4778574 began at 5.0±1.2 min and lasted until 20±6 min equating to projected $C_{b,u}$ of 0.98±0.23 and 0.35±0.09 nM, respectively, based on linear dose-$C_{b,u}$ extrapolation from the rat IV pharmacokinetics study (Figure 3B). Although the ability to block the PF-4778574 effects with a selective AMPAR antagonist (e.g. CP-465022 (Menniti et al.,

2003)) was not explored, other studies in this model have shown such antagonism to inhibit completely these same restorative effects of other AMPAR potentiators (Kiss et al., 2011b; internal Pfizer unpublished data). Conceptually, results in this assay provided the electrophysiological rationale for studying PF-4778574 in the nhp ketamine-disrupted SDR task since monosynaptic projection from the hippocampus/subiculum to the medial PFC contributes to working memory (Goldman-Rakic, 1994), and such dysfunction is implicated in the decreased cognitive performance of schizophrenia patients (Tamminga et al., 2010; Lisman, 2012).

Nonhuman Primate Ketamine-disrupted SDR Task. Single doses of PF-4778574 (0.001, 0.01 and 0.1 mg/kg, SC) were evaluated in nhp for its capacity to attenuate the working memory deficits induced by acutely disrupting glutamatergic synaptic transmission by the NMDAR antagonist ketamine. Complete details and context of this study are discussed in Roberts et al. (2010). Using the nhp pharmacokinetics studies for dose selection, pretreatment time and the projection of evaluated $C_{b,u}$, across a 100-fold dose range PF-4778574 did not alter animal function in the absence of ketamine co-administration, but did provide significant protection against ketamine-impaired performance at 0.01 mg/kg, SC. From an exposure perspective (Figure 3D), the data suggest a mean projected $C_{b,u}$ of 0.38 nM is effective in this model while 10-fold lower (0.038 nM) or higher (3.8 nM) $C_{b,u}$ are not. Consistent with pro-cognitive phenomenon (Lidow et al., 1998; Calabrese, 2008; Hutson et al., 2011), PF-4778574 demonstrated a hormetic exposure-response effect in this nhp model, although the true width of the "inverted U"-shaped dose-response curve is unknown without more granular dose selection between active and inactive doses.

Discussion

The AMPAR potentiator PF-4778574 was characterized in a series of in vitro assays and acute-dose animal studies evaluating AMPAR-mediated mechanism, safety and nootropism. Potentiator-induced animal effects were likely purely AMPAR-dependent since PF-4778574 (10 μM) only affected the dopamine transporter (IC_{50} of 910 nM) in a broad human-based receptor/enzyme selectivity panel (Cerep, 118 targets). For each animal dose, $C_{b,u}$ was calculated to define a $C_{b,u}$-normalized AMPAR-regulated interspecies exposure-response continuum for PF-4778574 to understand separations between $C_{b,u}$ enhancing cognition, disturbing motor coordination and triggering convulsion, as well as in vitro-in vivo pharmacological associations. Ultimately, these datasets provided a single-dose target-based TI for determining if PF-4778574 might be tested safely in humans.

Since it is unclear which AMPAR subtypes should (and/or can) be selectively targeted to balance optimally safety and efficacy, the in vitro characterization of PF-4778574 had a primary strategy of quantifying its pharmacological properties in rodent tissues that likely express native populations of AMPARs and their associated proteins. This subtype-independent approach was supported by nineteen AMPAR potentiators having similar functional potencies in mouse and human ES cell-derived neurons (McNeish et al., 2010), and it was evaluated further by determining if PF-4778574 caused equivalent effects at similar $C_{b,u}$ in rodents and large animals. Using the proprietary radioligand [^{3}H]PF-04725379 that binds at the same AMPAR allosteric site as biarylpropylsulfonamide LY451646 (Quirk and Nisenbaum, 2002), PF-4778574 had a mean K_i of 85 nM in a rat cortical homogenate. Functionally, PF-4778574 demonstrated

JPET Fast Forward. Published on July 30, 2013 as DOI: 10.1124/jpet.113.204735
This article has not been copyedited and formatted. The final version may differ from this version.

glutamate-dependent AMPAR positive allosteric modulation in mouse ES cell-derived neuronal precursors, rat primary cortical neurons and human GluA2-expressing homotetrameric systems (Table 1, Figure 2). For perspective, the benzamide potentiator CX516 (Arai and Kessler, 2007) did not displace [^{3}H]PF-04725379 and its functional assays' EC_{50} were >32 μM. Divergently, LY451646 had a K_i of 285 nM, mouse neuronal EC_{50} of 1.9 μM (McNeish et al., 2010) and human GluA2i EC_{50} of 117 nM. The cumulative in vitro data suggest PF-4778574 and LY451646 have a common AMPAR binding site, but PF-4778574 has similar functional potency at GluA2i and GluA2o.

Due to the convulsive risk of AMPAR potentiation (Yamada, 1998) and the unknown species-dependent dose-exposure correlation before exploratory experiments, animal studies predominately used subcutaneous administration to control the variability in C_{max} (and rise to it) and the potential confounds of a first-pass-generated active metabolite. Only dogs were orally dosed since these studies determined a maximally tolerated acute dose for chronic safety studies. In rodents, dogs and nhp, PF-4778574 demonstrated interneurocompartmental equilibria (Table 2), and the experimentally determined $C_{b,u}$:$C_{p,u}$ allowed the confident conversion of measured $C_{p,u}$ to $C_{b,u}$ when brain tissue was not excised for compound quantification. Additionally, in all species, only PF-4778574 was detected in brain homogenate suggesting it solely caused in vivo effects.

From a mechanism and safety perspective, PF-4778574 was first evaluated in mice for its ability to elevate cerebellar cGMP, a pharmacological event linked to AMPAR potentiation (Ryder et al., 2006). In this assay, PF-4778574 showed progressively greater statistically significant effects at mean $C_{b,u} \geq 1.7$ nM (Figure 5A). Equivalent cerebellar cGMP elevations at identical $C_{b,u}$ occurred in mice and rats with

JPET Fast Forward. Published on July 30, 2013 as DOI: 10.1124/jpet.113.204735
This article has not been copyedited and formatted. The final version may differ from this version.

LY451646 (Shaffer et al., 2009) suggesting similar AMPAR-mediated exposure-effect relationships in rodents. In mice, harmaline increases the potency of AMPAR potentiators to elevate cerebellar cGMP purportedly by enhancing excitatory neurotransmitters within the olivary-cerebellar synapse (Ryder et al., 2006). Based on this and the fact that harmaline causes essential tremor by disturbing olivocerebellar rhythmicity (Deuschl and Elble, 2000), it became important to evaluate the tremorgenic potential of PF-4778574, which would be clinically dose-capping. Thus, before large animal dosing, PF-4778574 was evaluated in mice undergoing an accelerating rotarod test where it caused motor deficits at a mean $C_{b,u}$ of 4.8 nM, ca. 3-fold the minimal cGMP-elevating $C_{b,u}$ (Figure 5B). Subsequently, PF-4778574 caused general tremors in dogs at a $C_{b,u}$ of 11.1±3.2 nM and movement-related tremors/ataxia in nhp at a $C_{b,u}$ of 15.9±8.4 nM (Figure 4A). Tremorgenic $C_{b,u}$ were consistent across dogs and nhp, and their mean values were ca. 2-to-3-fold the mouse rotarod $C_{b,u}$, which effectively overlapped with the lowest tremor-causing $C_{b,u}$ in dogs. Doses beyond those causing movement-related tremors/ataxia were tested in mice, rats and dogs, but not nhp, to evaluate convulsion liability (Figure 4B). Mice ($C_{b,u}$ of 11.6±4.0) and rats ($C_{b,u}$ of 11.2±1.6) had uniform convulsion thresholds, which were conserved in dogs (mean $C_{b,u}$ of 17.4 nM). Of note, no convulsion was self-limiting and rodent convulsions were not preceded by observable tremors. Holistically, the data suggest that PF-4778574 causes analogous adverse events at similar $C_{b,u}$ across species, and progressively higher $C_{b,u}$ lead from cerebellar cGMP elevation to motor coordination disruptions to convulsion.

AMPAR potentiators have demonstrated pro-cognitive effects in numerous animal models (Black, 2005) and small clinical trials (Marenco and Weinberger, 2006).

JPET Fast Forward. Published on July 30, 2013 as DOI: 10.1124/jpet.113.204735
This article has not been copyedited and formatted. The final version may differ from this version.

For this work, PF-4778574 was specifically evaluated in two models of pharmacologically induced NMDAR hypofunction to explore its ability to assuage glutamatergic dysregulation as it pertains to working memory impairment in schizophrenia. In a rat model (Kiss et al., 2011a; Kiss et al., 2011b) exploring the subiculum-medial PFC pathway, PF-4778574 overcame the disruptive effects of MK-801 on both cortical EEG and PPF at a projected $C_{b,u}$ of 0.715±0.276 nM (Figure 6A–B). This reversal is likely a direct effect of PF-4778574 as the initial MK-801-induced disruption returned once the mean $C_{b,u}$ fell below that (0.3 nM) maximally projected for the ineffective dose of 0.03 mg/kg (Figure 6C). Interestingly, genetically modified NMDAR hypomorphic mice display identical cortical and hippocampal EEG activities as observed in this rat model, and, as in rats, the AMPAR potentiator LY451395 normalized these electrophysiological signals at comparable $C_{b,u}$ (Kiss et al., 2013). This demonstrates AMPAR potentiation improves the impaired synaptic transmission and neuronal network oscillations in both pharmacological and genetic models of hypoglutamatergia. These rat electrophysiological data further rationalized studying PF-4778574 in the nhp ketamine-disrupted SDR task since monosynaptic projection from the hippocampus/subiculum to the PFC contributes to working memory (Goldman-Rakic, 1994), and such dysfunction may underlie the diminished cognitive performance of schizophrenia patients (Tamminga et al., 2010; Lisman, 2012). In this nhp model (Roberts et al., 2010), PF-4778574 did not affect spatial working memory performance in the absence of ketamine, but did block its impairing effects at a projected mean $C_{b,u}$ of 0.38 nM. Furthermore, PF-4778574 did not hinder the ketamine working memory disruptions at mean $C_{b,u}$ of 0.038 or 3.8 nM mirroring a hormetic exposure-response

relationship typical of nootropics (Lidow et al., 1998; Calabrese, 2008; Hutson et al., 2011). Data from both models suggest effects deemed pro-cognitive (i.e. "efficacy") either electrophysiologically or behaviorally occur at essentially equivalent $C_{b,u}$.

Due to the consistent $C_{b,u}$-effect relationships across multiple species, the datasets were integrated to afford a species-normalized AMPAR-mediated exposure-response continuum for PF-4778574 that provided an overall preclinical TI (Table 3). Cognitive effects occurred at $C_{b,u}$ of 0.38 to 0.72 nM, but were lost behaviorally in nhp between mean $C_{b,u}$ of 0.38 and 3.8 nM. Amid improved working memory emergence and disappearance, PF-4778574 significantly activated AMPARs within the cerebellum, as measured by cGMP elevation ($C_{b,u}$ of 1.7 nM), leading to motor coordination disruptions manifested as decreased rotarod fall latency in mice ($C_{b,u}$ of 4.8 nM), general tremors in dogs ($C_{b,u}$ of 11.1±3.2 nM) or movement-related tremors/ataxia in nhp ($C_{b,u}$ of 15.9±8.4 nM). Intriguingly, FDG-PET studies with LY451646 in rats (Zasadny et al., 2009) and nhp (Williams et al., 2009) demonstrated increased cerebral glucose metabolism rotating from cortical regions to the cerebellum at $C_{b,u}$ paralleling the behavioral transition from improved cognition to motor coordination disruption. Closely thereafter (mean $C_{b,u}$ $\geq$11.2 nM), the continuum completes with generalized convulsions in all species. From a mean exposure-response perspective, the data suggest a convulsion-based TI of 16–30 in rodents and 24–46 in dogs; for motor coordination disruptions, PF-4778574 has a TI of 7–13, 16–29 and 22–42 in mice, dogs and nhp, respectively.

Interestingly, the $C_{b,u}$ mediating physiological effects are just fractions of the concentrations required to produce half-maximal responses in the receptor-based in vitro assays (Table 1). Using the rat K_i and respective mean $C_{b,u}$ (Table 3), efficacy and

convulsion happen at projected AMPAR occupancies of <1% and 12–17%, respectively, and 30 nM PF-4778574 was the lowest tested concentration that clearly enhanced *S*-AMPA-evoked currents in rat cortical neurons (Figures 2A and 2C). A potential explanation for this phenomenon is that animals, unlike the utilized in vitro systems, have fully intact, synergistic neural networks where only minimal AMPAR potentiation affords enough excitatory neurotransmission for the non-linear activation of downstream pathways.

Assuming the single-dose-defined TI is not compressed upon chronic dosing and that both preclinical efficacy (mean $C_{b,u}$ of 0.38 to 0.72 nM) and the lowest large animal tremorgenic $C_{b,u}$ (6.00) are translatable, the described animal data suggest PF-4778574 has an 8-to-16-fold TI in humans for self-limiting tremor, a readily monitorable clinical adverse event. This TI, supplemented with projected human pharmacokinetic properties and their intersubject variability at a forecasted clinically efficacious dose (Shaffer et al., 2012), suggests PF-4778574 may be evaluated safely as a cognitive enhancer in patients with schizophrenia.

Acknowledgments

The authors acknowledge Dr. Kimberly Estep, Dr. Anton Fliri and Mr. Randall Gallaschun for the synthesis and purification of PF-4778574; Ms. Nandini Patel for compiling the synthesis and characterization data for PF-4778574; Mr. Curt Christoffersen for conducting the in-life portion of the nhp pharmacokinetics study; and, numerous colleagues within the department of Drug Safety and Research for conducting the dog single-dose escalation studies.

Authorship Contributions

Participated in research design: Bryce, Hajós, Hanks, Hoffmann, Hurst, Lotarski, Menniti, Schmidt, Scialis, Shaffer and Weber

Conducted experiments: Bryce, Hanks, Hoffmann, Lazzaro, Liu, Lotarski, Osgood, Scialis and Weber

Performed data analysis: Bryce, Hajós, Hanks, Hoffmann, Hurst, Lazzaro, Liu, Lotarski, Menniti, Osgood, Schmidt, Scialis, Shaffer and Weber

Wrote or contributed to the writing of the manuscript: Hajós, Hurst, Lazzaro, Menniti, Schmidt, Shaffer and Weber

References

Arai AC and Kessler M (2007) Pharmacology of Ampakine Modulators: From AMPA Receptors to Synapses and Behavior. *Curr Drug Targets* **8**:583-602.

Black MD (2005) Therapeutic Potential of Positive AMPA Modulators and Their Relationship to AMPA Receptor Subunits. A Review of Preclinical Data. *Psychopharmacology* **179**:154-163.

Calabrese EJ (2008) Alzheimer's Disease Drugs: An Application of the Hormetic Dose-Response Model. *Crit Rev Toxicol* **38**:419-451.

Collingridge GL, Volianskis A, Bannister N, France G, Hanna L, Mercier M, Tidball P, Fang G, Irvine MW, Costa BM, Monaghan DT, Bortolotto ZA, Molnar E, Lodge D and Jane DE (2013) The NMDA receptor as a target for cognitive enhancement. *Neuropharmacology* **64**:13-26.

Deuschl G and Elble R (2000) The pathophysiology of essential tremors. *Neurology* **54**:S14-S20.

Di L, Umland JP, Chang G, Huang Y, Lin Z, Scott DO, Troutman MD and Liston TE (2011) Species independence in brain tissue binding using brain homogenates. *Drug Metab Dispos* **39**:1270-1277.

Doran AC, Osgood SM, Mancuso JY and Shaffer CL (2012) An evaluation of using rat-derived single-dose neuropharmacokinetic parameters to project accurately large animal unbound brain drug concentrations. *Drug Metab Dispos* **40**:2162-2173.

Estep KG, Fliri AFJ and O'Donnell CJ (2008); Pfizer Inc., assignee. Sulfonamides and pharmaceutical compositions thereof. World patent WO2008120093A1. 26 Mar 2008.

Fleming JJ and England PM (2010) Developing a complete pharmacology for AMPA receptors: a perspective on subtype-selective ligands. *Bioorg Med Chem* **18**:1381-1387.

Garthwaite G and Garthwaite J (1991) Mechanisms of AMPA neurotoxicity in rat brain slices. *Eur J Neurosci* **3**:729-736.

Goff DC and Coyle JT (2001) The emerging role of glutamate in the pathophysiology and treatment of schizophrenia. *Am J Psychiatry* **158**:1367-1377.

Goldman-Rakic PS (1994) Working memory dysfunction in schizophrenia. *J Neuropsychiatry* **6**:348-357.

Grove SJA, Jamieson C, Maclean JKF, Morrow JA and Rankovic Z (2010) Positive allosteric modulators of the α-amino-3-hydroxy-5-methyl-4-isoxazolepropionic acid (AMPA) receptor. *J Med Chem* **53**:7271-7279.

Harms JE, Benveniste M, Maclean JKF, Partin KM and Jamieson C (2013) Functional analysis of a novel allosteric modulator of AMPA receptors derived from a structure-based drug design strategy. *Neuropharmacology* **64**:45-52.

Hutson PH, Finger EN, Magliaro BC, Smith SM, Converso A, Sanderson PE, Mullins D, Hyde LA, Eschle BK, Turnbull Z, Sloan H, Guzzi M, Zhang X, Wang A, Rindgen D, Mazzola R, Vivian JA, Eddins D, Uslaner JM, Bednar R, Gambone C, Le-Mair W, Marino MJ, Sachs N, Xu G and Parmentier-Batteur S (2011) The selective phosphodiesterase 9 (PDE9) inhibitor PF-04447943 (6-[3*S*,4*S*)-4-methyl-1-(pyrimidin-2-ylmethyl)pyrrolidin-3-yl]-1-(tetrahydro-2*H*-pyran-4-yl)-1,5-dihydro-4*H*-pyrazolo[3,4-*d*]pyrimidin-4-one) enhances synaptic plasticity and cognitive function in rodents. *Neuropharmacology* **61**:665-676.

Javitt DC (2007) Glutamate and schizophrenia: phencyclidine, N-methyl-D-aspartate receptors, and dopamine-glutamate interactions. *Int Rev Neurobiol* **78**:69-108.

Kiss T, Feng J, Hoffman WE, Shaffer CL and Hajos M (2013) Rhythmic theta and delta activity of cortical and hippocampal neuronal networks in genetically or pharmacologically induced NMDA receptor hypofunction under urethane anesthesia. *Neuroscience* **237**:255-267.

Kiss T, Hoffman WE, Scott L, Kawabe TT, Milici AJ, Nilsen EA and Hajos M (2011a) Role of thalamic projection in NMDA receptor-induced disruption of cortical slow oscillation and short-term plasticity. *Front Psychiatry* **2**:1-12.

Kiss T, Hoffmann WE and Hajos M (2011b) Delta oscillation and short-term plasticity in the rat medial prefrontal cortex: modelling NMDA hypofunction of schizophrenia. *Int J Neuropsychopharmacol* **14**:29-42.

Krystal JH, Karper LP, Seibyl JP, Freeman GK, Delaney R, Bremner JD, Heninger GR, Bowers J, M.B. and Charney DS (1994) Subanesthetic effects of the noncompetitive NMDA antagonist, ketamine, in humans. Psychotomimetic, perceptual, cognitive, and neuroendocrine responses. *Arch Gen Psychiatry* **51**:199-214.

Lidow MS, Williams GV and Goldman-Rakic PS (1998) The Cerebral Cortex: A Case for a Common Site of Action of Antipsychotics. *TiPS* **19**:136-140.

Lisman J (2012) Excitation, inhibition, local oscillations, or large-scale loops: what causes the symptoms of schizophrenia? *Curr Opin Neurobiol* **22**:537-544.

Liu X, Van Natta K, Yeo H, Vilenski O, Weller PE, Worboys PD and Monshouwer M (2009) Unbound drug concentration in brain homogenate and cerebral spinal fluid at steady state as a surrogate for unbound concentration in brain interstitial fluid. *Drug Metab Dispos* **37**:787-793.

Lynch G (2002) Memory enhancement: the search for mecahnism-based drugs. *Nat Neurosci* **5**:1035-1038.

Lynch G and Gall CM (2006) Ampakines and the Threefold Path to Cognitive Enhancement. *Trends Neurosci* **29**:554-562.

Malinow R and Malenka RC (2002) AMPA receptor trafficking and synaptic plasticity. *Ann Rev Neurosci* **25**:103-126.

Marenco S and Weinberger DR (2006) Therapeutic Potential of Positive AMPA Receptor Modulators in the Treatment of Neuropsychiatric Disorders. *CNS Drugs* **20**:173-185.

McNeish J, Roach M, Hambor J, Mather RJ, Weibley L, Lazzaro J, Gazard J, Schwarz J, Volkmann R, Machacek D, Stice S, Zawadzke L, O'Donnell C and Hurst R (2010) High-throughput screening in embryonic stem cell-derived neurons identifies potentiators of α-amino-3-hydroxyl-5-methyl-4-isoxazolepropionate-type glutamate receptors. *J Biol Chem* **285**:17209-17217.

Meador-Woodruff JH and Healy DJ (2000) Glutamate receptor expression in schizophrenic brain. *Brain Res Rev* **31**:288-294.

Menniti FS, Buchan AM, Chenard BL, Critchett DJ, Ganong AH, Guanowsky V, Seymour PA and Welch WM (2003) CP-465,022, a selective noncompetitive AMPA receptor antagonist, blocks AMPA receptors but is not neuroprotective in vivo. *Stroke* **34**:171-176.

Millan MJ, Agid Y, Brune M, Bullmore ET, Carter CS, Clayton NS, Connor R, Davis S, Deakin B, DeRubeis RJ, Dubois B, Geyer MA, Goodwin GM, Gorwood P, Jay TM, Joels M, Mansuy IM, Meyer-Lindenberg A, Murphy D, Rolls E, Saletu B, Spedding M, Sweeney J, Whittington M and Young LJ (2012) Cognitive dysfunction in psychiatric disorders: characteristics, causes and the quest for improved therapy. *Nat Rev Drug Discov* **11**:141-168.

Moghaddam B and Javitt DC (2012) From revolution to evolution: the glutamate hypothesis of schizophrenia and its implication for treatment. *Neuropsychopharmacol Rev* **37**:4-15.

Morris RGM (2003) Long-term potentiation and memory. *Philos Trans R Soc Lond B Biol Sci* **358**:643-647.

O'Neill MJ, Bleakman D, Zimmerman DM and Nisenbaum ES (2004) AMPA Receptor Potentiators for the Treatment of CNS Disorders. *Curr Drug Targets* **3**:181-194.

Olney JW and Farber NB (1995) Glutamate receptor dysfunction and schizophrenia. *Arch Gen Psychiatry* **52**:998-1007.

Olney JW, Newcomer JW and Farber NB (1999) NMDA receptor hypofunction model of schizophrenia. *J Psychiatr Res* **33**:523-533.

Parsons CG, Danysz W and Zieglgansberger W (2005) Excitatory amino acid neurotransmission *Handb Exp Pharmacol* **169**:249-303.

Quirk JC and Nisenbaum ES (2002) LY404187: A Novel Positive Allosteric Modulator of AMPA Receptors. *CNS Drug Rev* **8**:255-282.

Roberts BM, Holden DE, Shaffer CL, Seymour PA, Menniti FS, Schmidt CJ, Williams GV and Castner SA (2010) Prevention of ketamine-induced working memory impairments by AMPA potentiators in a nonhuman primate model of cognitive dysfunction. *Behav Brain Res* **212**:41-48.

Ryder JW, Falcone JF, Manro JR, Svensson KA and Merchant KM (2006) Pharmacological Characterization of cGMP Regulation by the Biarylpropylsulfonamide Class of Positive, Allosteric Modulators of α-Amino-3-hydroxy-5-methyl-4-isoxazolepropionic Acid Receptors. *J Pharmacol Exp Ther* **319**:293-298.

Shaffer CL (2010) Defining neuropharmacokinetic parameters in CNS drug discovery to determine cross-species pharmacologic exposure-reponse relationships. *Annu Rep Med Chem* **45**:55-69.

Shaffer CL, Scialis RJ, Lotarski S, Bryce DK, Liu J, Majchrzak MJ, Christoffersen C, Hoffmann WE, Campbell B, Hurst RS, McLean S, Ganong AH, Hajos M, Seymour PA, Menniti FS and Schmidt CJ (2009) Defining the mechanism-mediated exposure-response continuum of a novel AMPA receptor potentiator. *Soc Neurosci Abstr* 883.17.

Shaffer CL, Scialis RJ, Rong H and Obach RS (2012) Using Simcyp to project human oral pharmacokinetic variability in early drug research to mitigate mechanism-based adverse events. *Biopharm Drug Dispos* **33**:72-84.

Sun X, Zhao Y and Wolf ME (2005) Dopamine receptor stimulation modulates AMPA receptor synaptic insertion in prefrontal cortex neurons. *J Neurosci* **25**:7342-7351.

Tamminga CA, Stan AD and Wagner AD (2010) The hippocampal formation in schizophrenia. *Am J Psychiatry* **167**:1178-1193.

Tillement J-P, Urien S, Chaumet-Riffaud P, Riant P, Bree F, Morin D, Albengres E and Barre J (1988) Blood binding and tissue uptake of drugs. Recent advances and perspectives. *Fundam Clin Pharmacol* **2**:223-238.

Williams GV, Roberts BM, Holden DE, Campbell DW, Shaffer CL, Scialis RJ, Seymour PA, Menniti FS, Schmidt CJ, Sandiego CM, Carson RE and Castner SA (2009) Cerebral metabolic correlates of ketamine-induced cognitive deficits and their reversal by a positive allosteric modulator of the AMPA receptor: a functional imaging study in the nonhuman primate using FDG-PET. *Soc Neurosci Abstr* 748.10.

Yamada KA (1998) Modulating excitatory synaptic neurotransmission: potential treatment for neurological disease. *Neurobiol Dis* **5**:67-80.

Zarate Jr. CA and Manji HK (2008) The role of AMPA receptor modulation in the treatment of neuropsychiatric diseases. *Exp Neurol* **211**:7-10.

Zasadny K, Callahan MJ, Kuszpit K, Chen L, Skaddan M, Brown-Proctor C, Harris R, Zhu A, Shaffer CL and Scialis RJ (2009) FDG-PET imaging provides insights into efficacy and safety for an AMPA receptor potentiator. *World Mol Imaging Soc Abstr* 909.

Footnote

Current addresses:

[1]Amgen Inc., Cambridge, MA

[2]Bristol-Myers Squibb Company, Wallingford, CT

[3]Mnemosyne Pharmaceuticals, Inc., Providence, RI

[4]Yale School of Medicine, New Haven, CT

Legends for Figures

Figure 1. Chemical structure of PF-4778574.

Figure 2. Summary of the electrophysiology experiments in rat primary cortical neurons. Panel A: PF-4778574 (3 to 3000 nM, N=7–9 cells/concentration) concentration-response relationship at a fixed concentration (30 μM) of *S*-AMPA. Panel B: The *S*-AMPA (0.1 to 100 μM) concentration-response relationship in the absence (●, N=8 cells/concentration) or presence (○, N=6 cells/concentration) of PF-4778574 (300 nM). Panel C: Exemplified current traces used to generate the concentration-response data within Panel A.

Figure 3. Summary of the species-specific exposure-time data following a single dose of PF-4778574. Panel A: Mean $C_{p,u}$ (▲), C_{CSF} (■) and $C_{b,u}$ (○) vs. time in rats (1 mg/kg, SC). Panels B, C and D: Mean projected $C_{b,u}$ vs. time in rats (0.2 mg/kg, IV, ○), dogs (0.1 (○), 0.2 (●) and 0.25 (□) mg/kg, PO) and nhp (0.1 (○) and 0.32 (●) mg/kg, SC), respectively. In Panel B, mean ± SD projected $C_{b,u}$ are plotted due to N=3/time point; all other graphs lack SD due to N≤2/time point.

Figure 4. Summary of the species-specific exposure-adverse event data following a single dose of PF-4778574. Panel A: Tremorgenic projected $C_{b,u}$ in individual dogs (0.2 (○) and 0.25 (□) mg/kg, PO) and nhp (0.32 mg/kg, SC (○)). Filled symbols designate intraanimal means. Panel B: Convulsion-causing $C_{b,u}$ (○) in individual CD-1 mice (N=11), rats (N=11) and dogs (N=2). Filled symbols designate interanimal means.

JPET Fast Forward. Published on July 30, 2013 as DOI: 10.1124/jpet.113.204735
This article has not been copyedited and formatted. The final version may differ from this version.

Figure 5. PF-4778574 dose-dependently increased CD-1 mouse cerebellum cGMP (panel A) and decreased fall latency in C57BL/6J mice traversing an accelerating rotarod (panel B). For both assays, single doses were administered subcutaneously with a 0.5 h pretreatment time; for each dose, the projected mean $C_{b,u}$ at 0.5 h after PF-4778574 administration is shown within brackets. The data are expressed as mean ± SEM with N=5–6/dose (cGMP) or N=12/dose (rotarod). * P<0.05, ** P<0.01; One-way ANOVA followed by *post hoc* Dunnett's *t* test.

Figure 6. Summary of the exposure-response relationship in the rat MK-801-disrupted cortical oscillation and paired-pulse facilitation (PPF) assay following IV administration of PF-4778574. Panels A and B: Typical recordings of local field potentials (EEG, panel A) and evoked field potentials (PPF, panel B) in the medial PFC of an anesthetized rat under control condition, and after chronologic administration of MK-801 (0.05 mg/kg, IV) and PF-4778574 (0.1 mg/kg, IV), respectively. In the control condition, local field potential was characterized by a regular ca. 2 Hz delta oscillation and PPF in response to a pair of stimulation pulses delivered in the subiculum. The MK-801-induced disruption in both regular delta oscillation and decline in PPF were reversed by PF-4778574. Panel C: Summary of the reversal action of PF-4778574 on the MK-801-mediated reduction in PPF. Each column represents PPF values (mean ± SEM, N=5) collected over a 10 min period, arrows designate compound administration. The projected mean $C_{b,u}$ for each time period post-dose is shown within brackets. * P<0.05 vs. control condition, # P<0.05 vs. MK-801 condition; Two-tailed Student's *t* test.

JPET Fast Forward. Published on July 30, 2013 as DOI: 10.1124/jpet.113.204735
This article has not been copyedited and formatted. The final version may differ from this version.

Tables

Table 1. Summary of primary in vitro pharmacology of PF-4778574 (mean ± SEM)

Binding Assay	pK_i (M)	K_i (nM)	Efficacy (%)	*N*
rat cortical tissue	7.07 ± 0.11	85	na	20
Functional Assay	**pEC_{50} (M)**	**EC_{50} (nM)**	**Efficacy (%)**	***N***
mES cell-derived neurons	6.04 ± 0.19	919	162 ± 24	7
hGluA2i	7.35 ± 0.11	45	111 ± 6	7
hGluA2o	7.05 ± 0.07	90	112 ± 5	5

na, not applicable; mES, mouse embryonic stem; h, human; i, flip; o, flop.

JPET Fast Forward. Published on July 30, 2013 as DOI: 10.1124/jpet.113.204735
This article has not been copyedited and formatted. The final version may differ from this version.

Table 2. Summary of interspecies brain penetration of PF-4778574

Species	Parameter	
	C_b:C_p [a]	$C_{b,u}$:$C_{p,u}$ [b]
Mouse[c]	1.24	0.42
Rat[d]	1.07	0.44
Dog[d]	1.35	0.51
nhp[d]	2.82	0.73

[a]Total brain compound concentration-to-total plasma compound concentration ratio.

[b]Unbound brain compound concentration-to-unbound plasma compound concentration ratio.

[c]Values are means of those determined in CD-1 and C57BL6/J mice.

[d]Species-specific values reported in Doran *et al.* (2012).

JPET Fast Forward. Published on July 30, 2013 as DOI: 10.1124/jpet.113.204735
This article has not been copyedited and formatted. The final version may differ from this version.

Table 3. Summary of the interspecies exposure-response continuum for PF-4778574

Response		$C_{b,u}$ (nM)			
		Mouse	Rat	Dog	nhp
Safety	Convulsion	11.6 ± 4.0	11.2 ± 1.6	17.4	—
	Tremor	nd	nd	11.1 ± 3.2	15.9 ± 8.4
	Rotarod	4.78	—	—	—
Mechanism	cGMP	1.70	—	—	—
Efficacy	PPF	—	0.715 ± 0.276	—	—
	SDR	—	—	—	0.380

—, not determined; nd, not detected; cGMP, cerebellum cGMP assay; PPF, MK-801-disrupted cortical oscillation and paired-pulse facilitation assay; SDR, ketamine-disrupted spatial delayed response task.

Figure 1

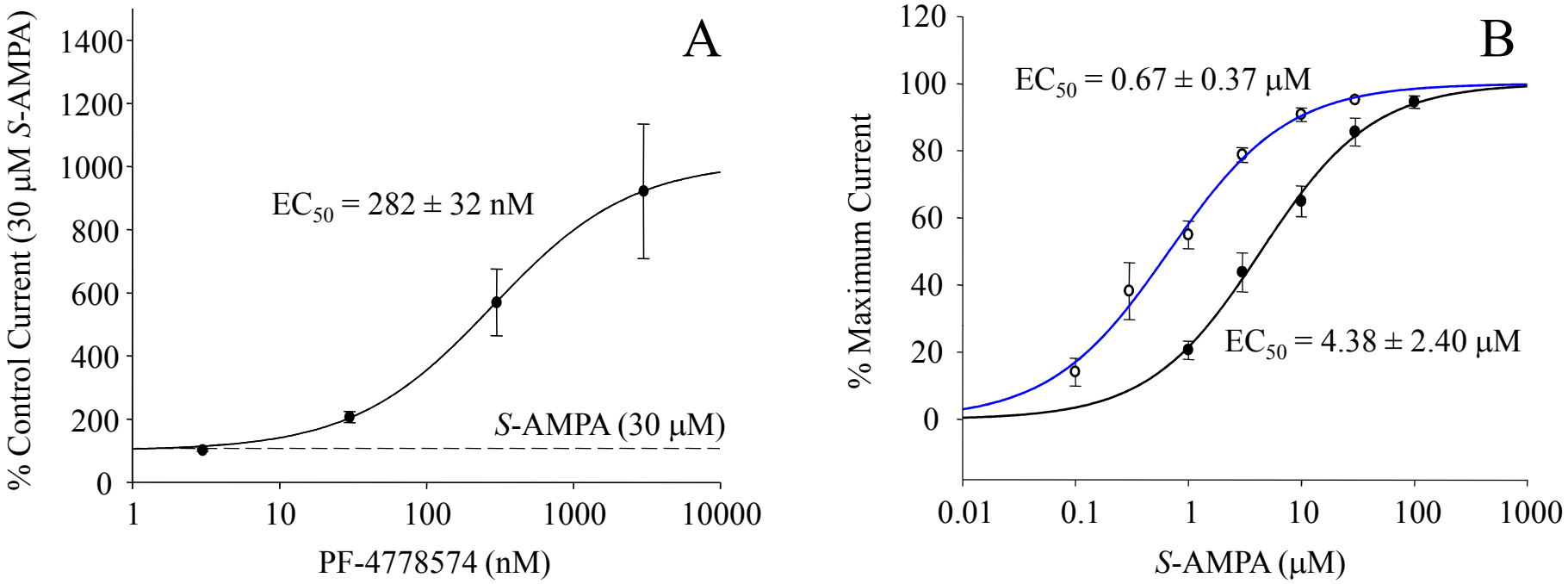

Figure 2, panels A and B

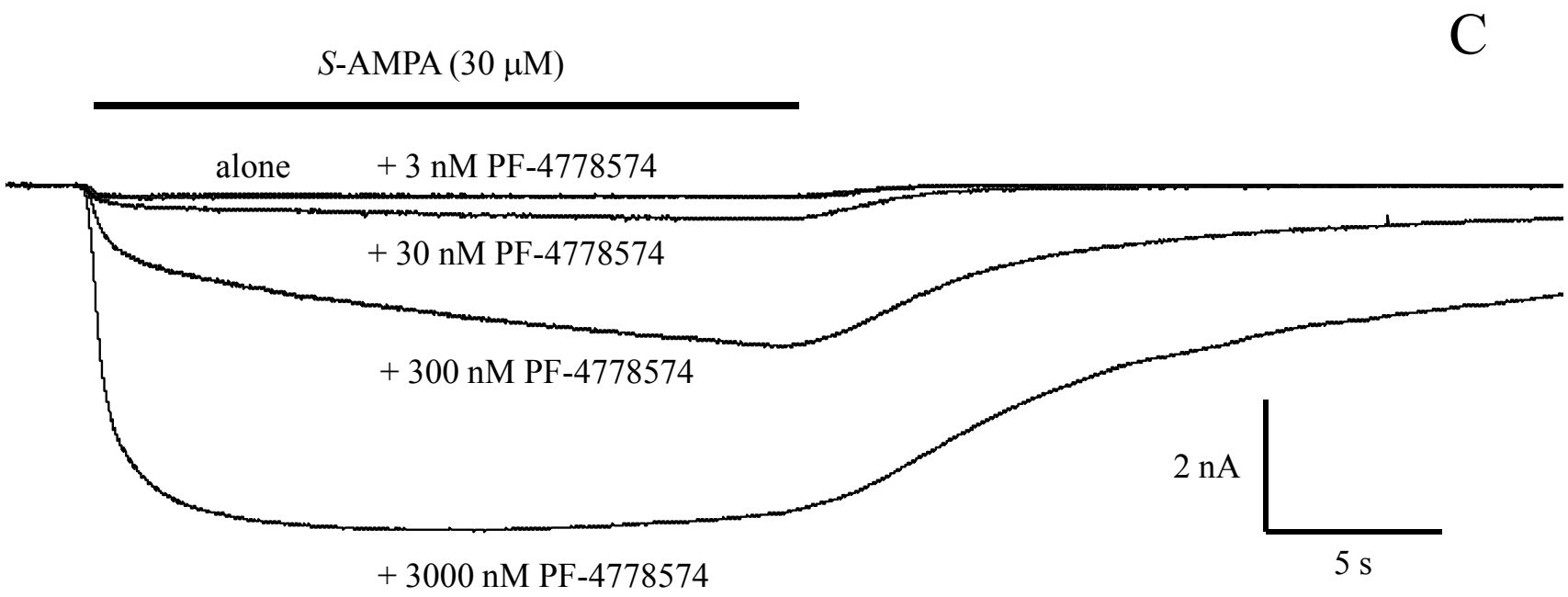

Figure 2, panel C

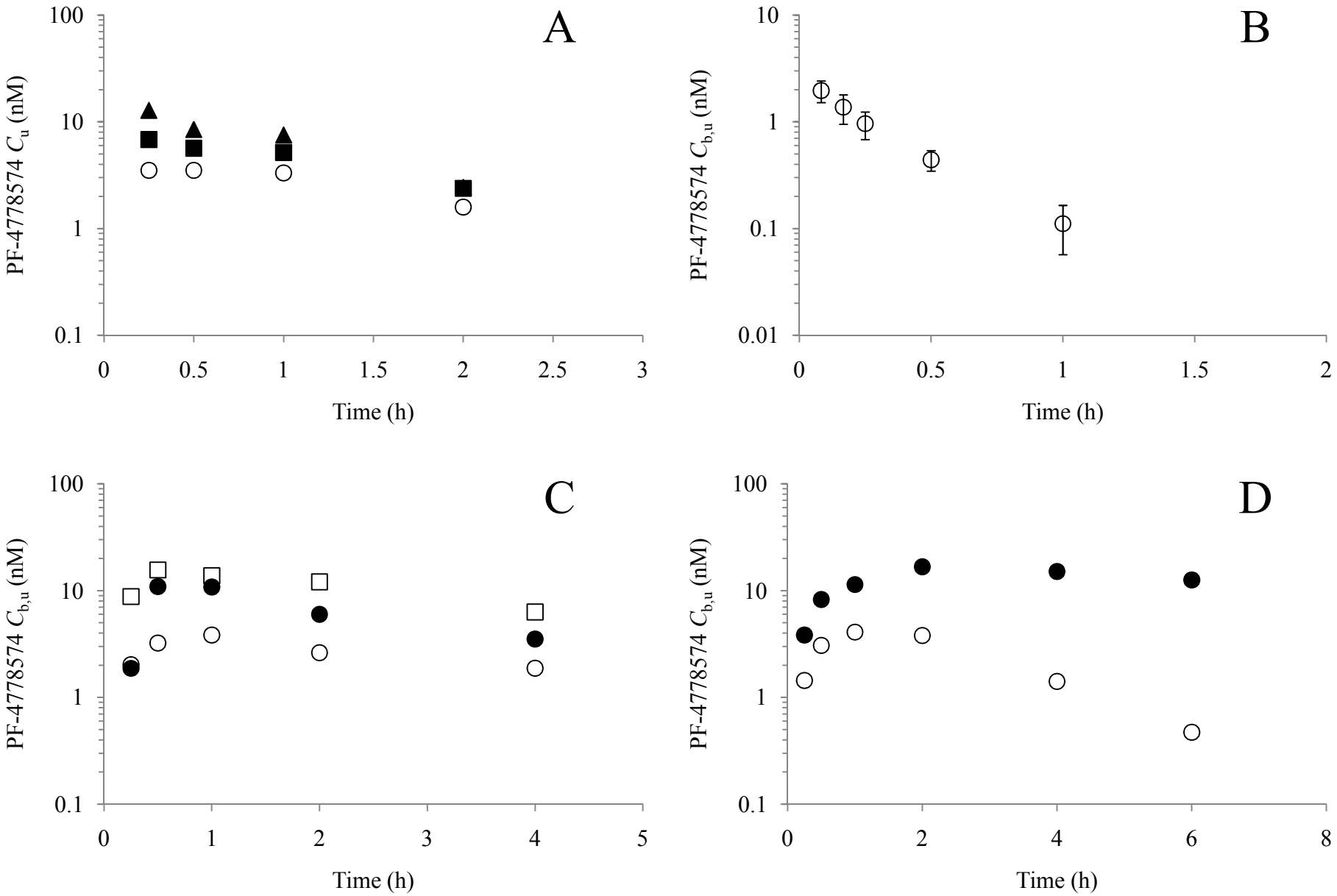

Figure 3

JPET Fast Forward. Published on July 30, 2013 as DOI: 10.1124/jpet.113.204735
This article has not been copyedited and formatted. The final version may differ from this version.

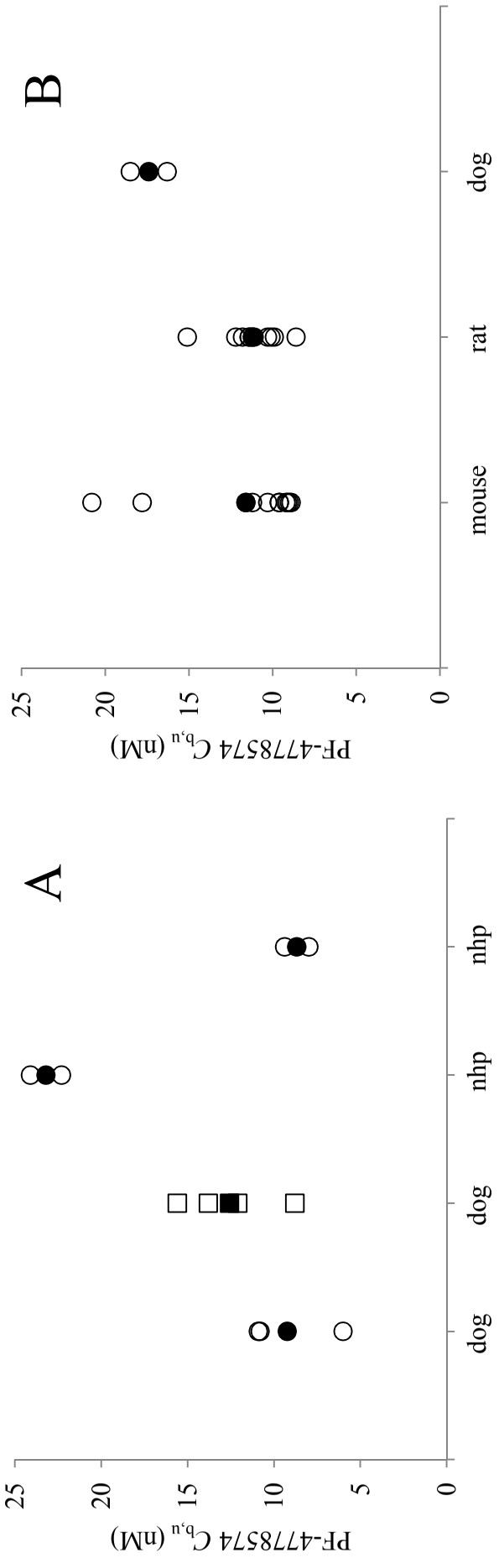

Figure 4

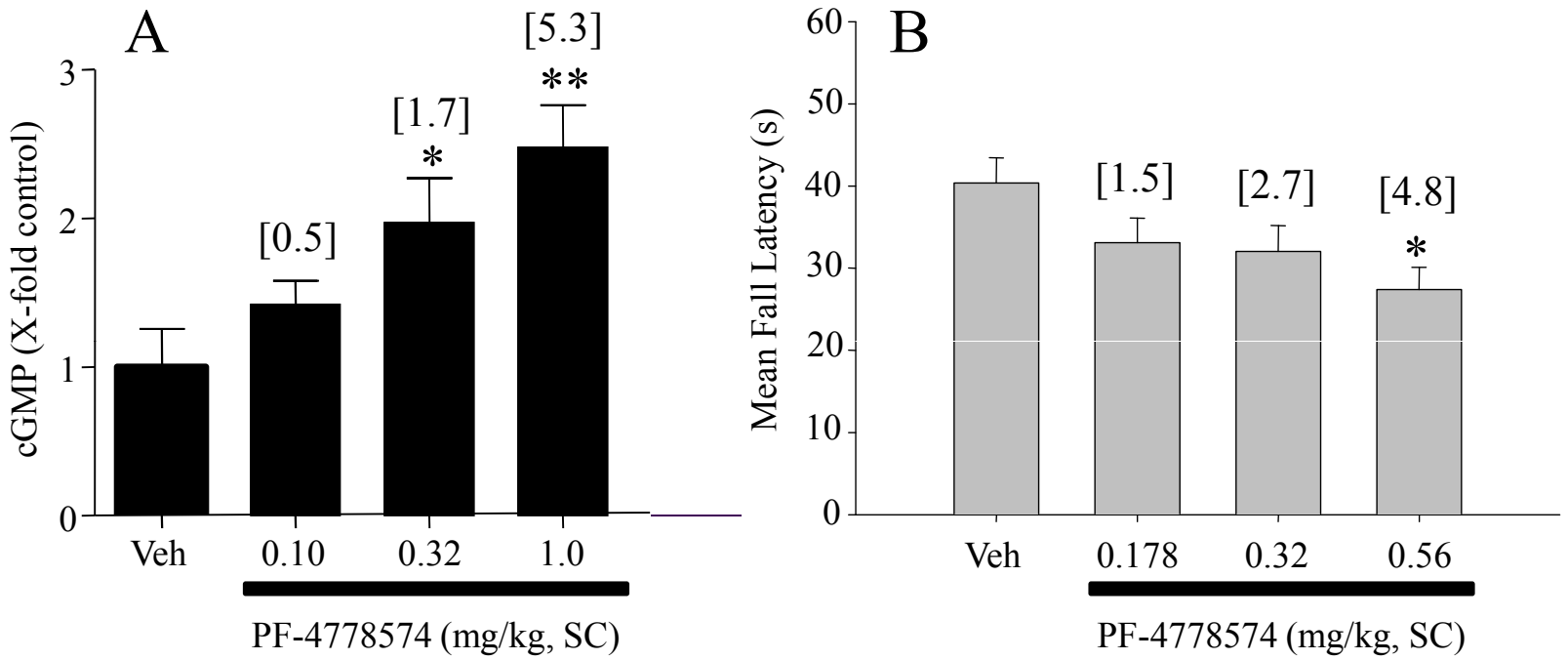

Figure 5

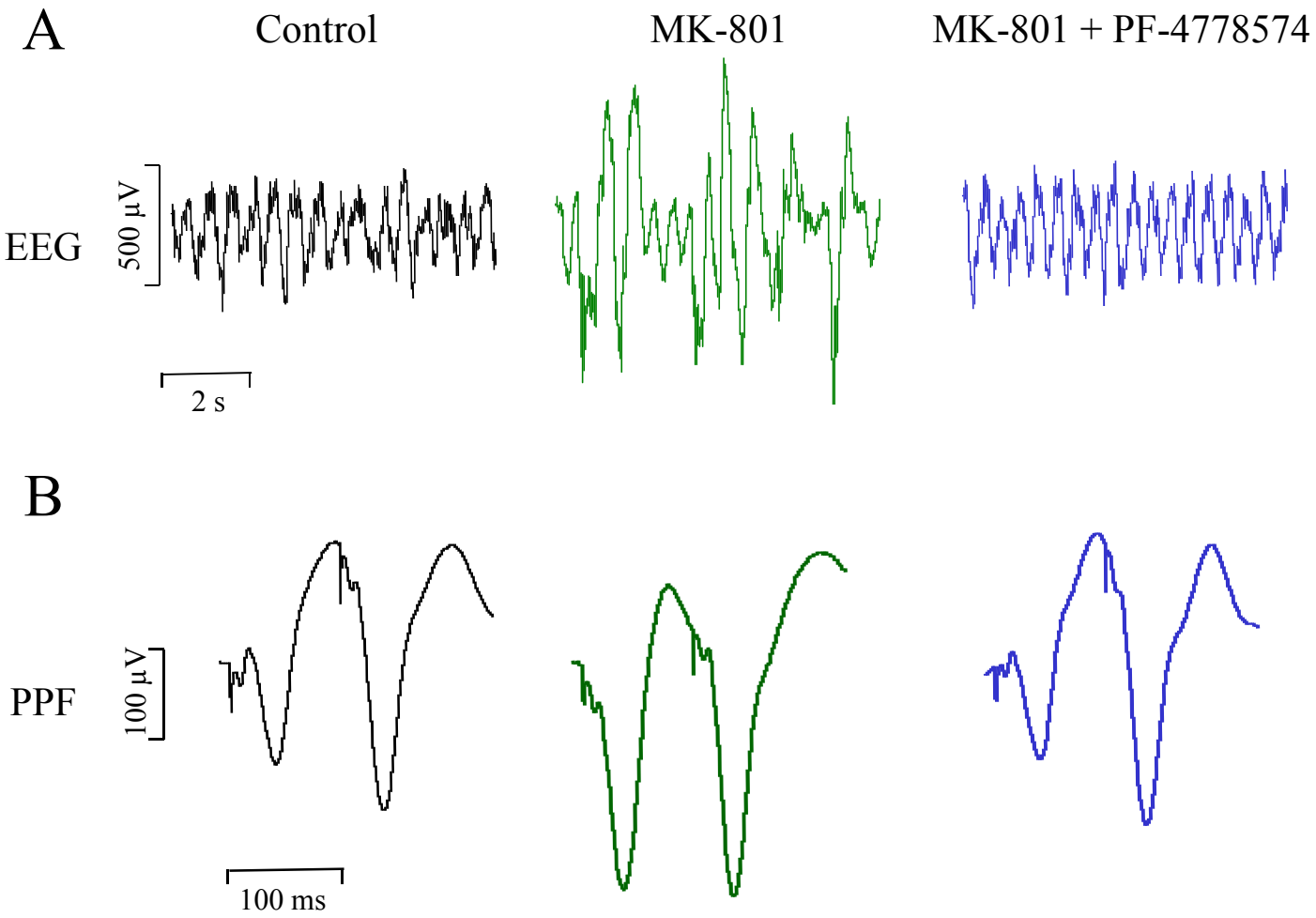

Figure 6, panels A and B

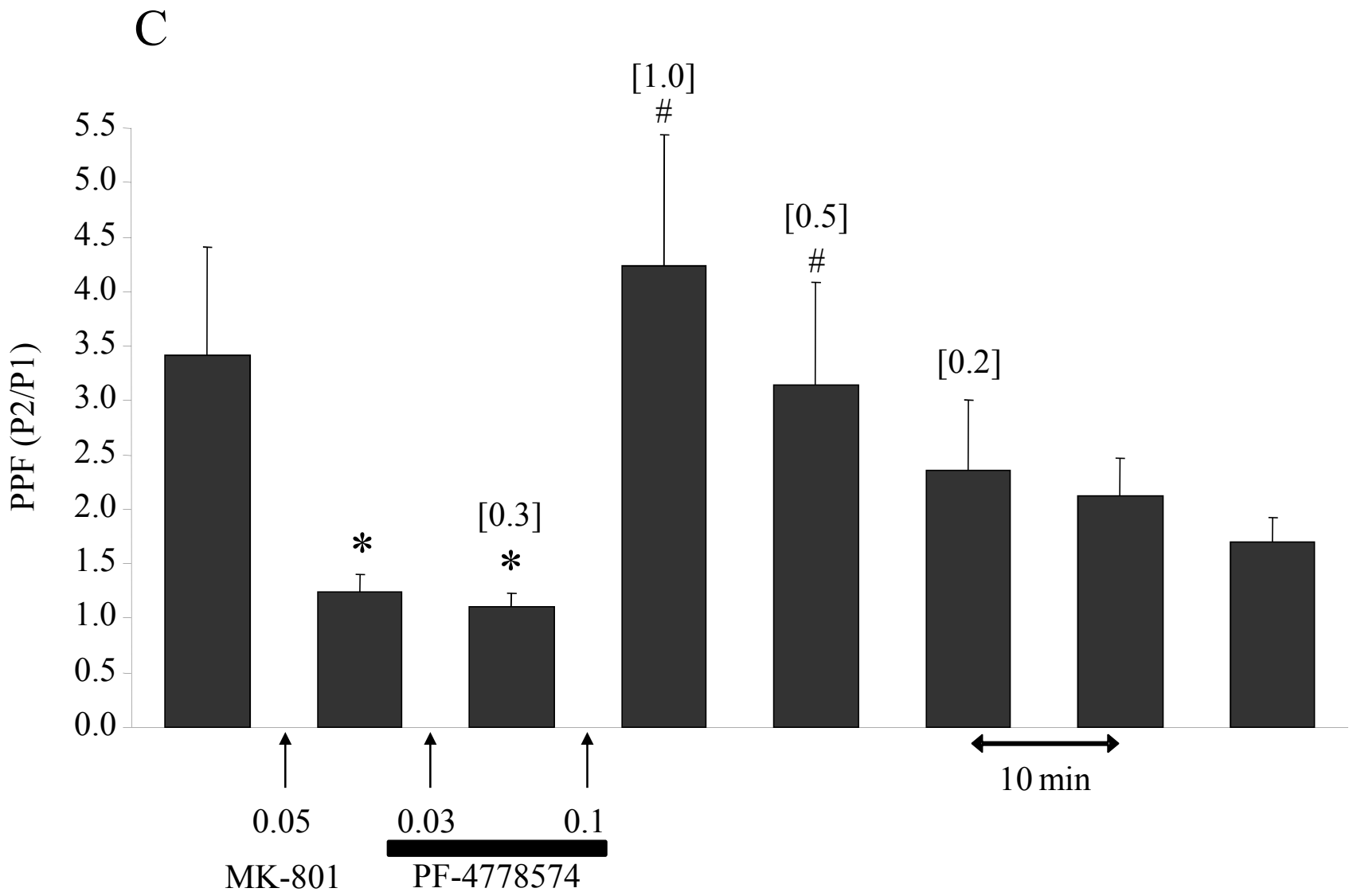

Figure 6, panel C